Neurons Speak in Ranges: Breaking Free from Discrete Neuronal Attribution

Anonymous authors
Paper under double-blind review

Abstract

Pervasive polysemanticity in large language models (LLMs) undermines discrete neuron–concept attribution, posing a significant challenge for model interpretation and control. We systematically analyze both encoder and decoder based LLMs across diverse datasets, and observe that even highly salient neurons for specific semantic concepts consistently exhibit *polysemantic* behavior. Importantly, we uncover a consistent pattern: concept-conditioned activation magnitudes of neurons form distinct, often Gaussian-like distributions with minimal overlap. Building on this observation, we hypothesize that interpreting and intervening on concept-specific activation ranges can enable more precise interpretability and targeted manipulation in LLMs. To this end, we introduce NeuronLens, a novel range-based interpretation and manipulation framework, that localizes concept attribution to activation ranges within a neuron. Extensive empirical evaluations show that *range-based interventions* enable effective manipulation of target concepts while causing substantially less collateral degradation to auxiliary concepts and overall model performance compared to neuron-level masking.

1 Introduction

Neuron interpretation aims to uncover how individual neurons encode semantic concepts and contribute to model outputs. Recent work has made significant progress in this direction by identifying neurons that are strongly associated with specific concepts or model behavior (Dalvi et al., 2019a; Antverg & Belinkov, 2022; Conmy et al., 2023; Marks et al., 2024). Common approaches include maximal activation analysis (Foote et al., 2023; Frankle & Carbin, 2019), which links neurons to inputs that produce the highest activations, probe-based methods (Dalvi et al., 2019a;b) that employ auxiliary classifiers to assess neuron–concept associations, and probeless approaches (Antverg & Belinkov, 2022) that infer such associations directly from neuron activations.

These methods typically rely, explicitly or implicitly, on discrete neuron-to-concept mappings, assuming that entire neurons encode single concepts. However, neurons frequently exhibit polysemanticity; the ability to encode multiple, seemingly unrelated concepts (Lecomte et al., 2024; Marshall & Kirchner, 2024). Given this heterogeneous encoding of concepts, traditional approaches can lead to unintended consequences when manipulating neurons, as changes intended for one concept may inadvertently affect others encoded by the same neuron, and suboptimal interpretations of concepts (Sajjad et al., 2022).

To better understand how polysemanticity manifests at the neuron level, we conduct a systematic analysis of neuron activations in both encoder- and decoder-based LLMs across multiple datasets. Focusing on neurons identified as salient for specific concepts, we observe that these neurons consistently exhibit polysemantic behavior, often responding to multiple concepts. Through qualitative and quantitative analysis, we further discover that concept-conditioned neuronal activation magnitudes form *Gaussian-like distributions*, with minimal overlap across different concepts. This observation suggests that although individual neurons are polysemantic, the activations associated with a given concept tend to concentrate within a specific band of activation magnitudes. That is, each concept is typically expressed within a characteristic activation range of a neuron, even when the same neuron participates in encoding multiple concepts.
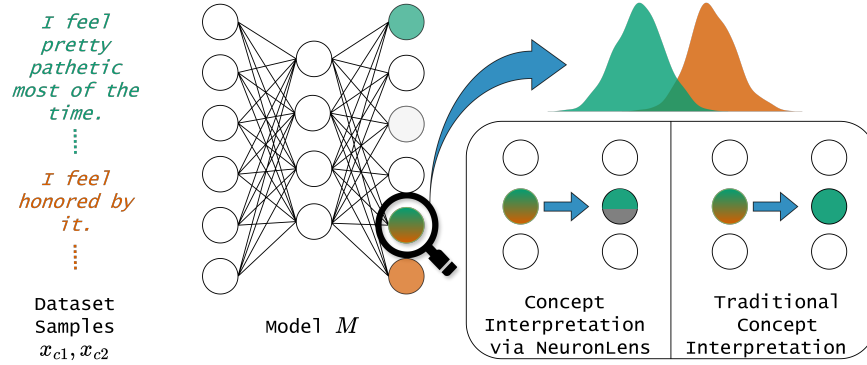
Figure 1: Different concepts induce distinct, Gaussian-like activation distributions within the same neuron, enabling range-based concept attribution and intervention.

Building on this observation, we introduce NeuronLens, a range-based attribution framework for neuron interpretation and manipulation, illustrated in Figure 1. Rather than attributing an entire neuron to a single concept, NeuronLens identifies and maps specific activation ranges within a neuron's distribution to individual concepts. Specifically, for a given concept, NeuronLens calculates an activation range that captures the majority of concept-conditioned activations, enabling precise attribution, which in turn allows for interventions that operate selectively within this range while leaving other activation regimes of the neuron unaffected. To causally validate our approach, we run extensive concept-erasure experiments. Across settings, our method reduces unintended interference on auxiliary concepts by up to 25 percentage points (-14 on Llama) than full neuron masking. Additionally, our range-based interventions preserve general capabilities of models, maintaining or improving performance on MMLU benchmark in most settings, while incurring only minor increases in language modeling perplexity on Wikipedia text.

Our work makes the following contributions. (1) We show that neuronal activations in LLMs form concept-conditioned, Gaussian-like distributions, with often exhibiting limited overlap across concepts. (2) We empirically demonstrate that concept-specific activation ranges are consistently identifiable within polysemantic neurons, providing a more fine-grained handle for neuron-level interpretation than discrete neuron-to-concept attribution. (3) We introduce NeuronLens to interpret and causally validate concept-specific activation ranges for targeted interventions, enabling precise manipulation of target concepts while reducing unintended interference compared to neuron-level masking.

2 Neuron Interpretation Analysis

2.1 Preliminaries

Neuron. We refer to the output of an activation as a neuron. In a transformer model, we consider neurons of hidden state vectors of different transformer layers. Formally, given a hidden state vector $\mathbf{h}^l \in \mathbb{R}^d$ of size d produced by layer l, h_j^l denotes its j-th neuron, i.e., the j-th component of $\mathbf{h}^l$.

Concept. A concept $c \in C$ is a high-level semantic category that groups each input instance (or components of every instance), where C is the set of all concepts. For example, in a language task, a sentence can be categorized into four types: declarative, interrogative, imperative, and exclamatory, where each type is a concept. Words in a sentence can also convey concepts such as nouns, verbs, adjectives, adverbs, and more. We study settings where all inputs are labeled with concepts.

Saliency Ranking. A saliency ranking orders the importance of neurons based on some saliency metric. For a hidden state vector $\mathbf{h}^l$, we denote the value of the saliency metric for the j-th neuron with respect to a concept c as s_j^c. The saliency ranking $(r_c(1), r_c(2), \cdots, r_c(d))$ is a permutation of the indices of neurons $(1, 2, \cdots, d)$, where $r_c(j) < r_c(i)$ if $s_j^c > s_i^c$. The saliency metric is usually predefined, such as absolute neuron activation values.
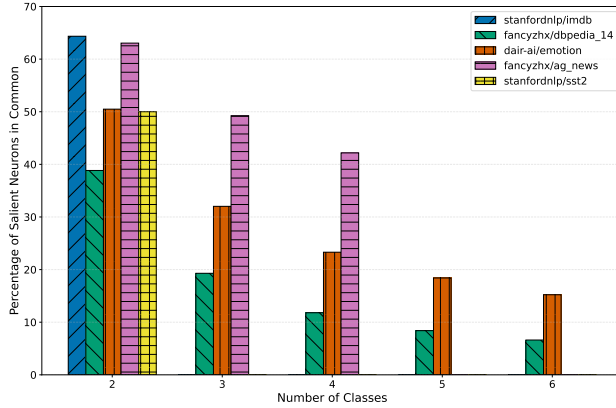
Figure 2: Overlap in top 30% salient neurons in GPT-2 model across classes in various datasets.

Concept Learning. Given a hidden state vector $\mathbf{h}^l$ as input, the associated concept can be the output of an appended neural network (e.g., several fully connected layers). The parameters of this appended neural network can be trained using training samples labeled with concepts.

2.2 Datasets and Models

Datasets. For various experiments in this work, we utilize the following datasets: sentiment analysis (IMDB (Maas et al., 2011)), (SST2 (Socher et al., 2013)), emotion detection (Dair-Ai/Emotions (Saravia et al., 2018)), news classification (AG-News (Zhang et al., 2015)), and article content categorization (DBPedia-14 (Zhang et al., 2015)). Moreover, we use the MMLU benchmark (Hendrycks et al., 2021) to evaluate general capabilities of LLMs and Wikipedia texts (Foundation) for open-ended generation.

Models. This work employs both encoder and decoder-based models, including pretrained Llama-3.2-3B (Grattafiori, 2024), fine-tuned BERT (Devlin et al., 2019), DistilBERT (Sanh et al., 2020), and GPT-2 (Radford et al., 2019).

2.3 Salient Neurons Extraction

We record activations for training samples of different concepts to perform neuron interpretation. Specifically, if we want to interpret neurons of $\mathbf{h}^l$ (hidden vector at layer l), we perform a forward pass using the training dataset and store the values of $\mathbf{h}^l$ and the associated concepts of all samples into a set H^l. The set H^l is further partitioned into H_c^l for all concepts $c \in C$. Such preparation is common in the relevant literature (Dalvi et al., 2019c;b; Antverg & Belinkov, 2022).

We explore standard neuron saliency approaches, namely max activations (Frankle & Carbin, 2019), prob-less (Antverg & Belinkov, 2022), and probe analysis (Dalvi et al., 2019b). Details of these approaches are provided in Appendix C. To evaluate these saliency methods, we employ a concept erasure task that masks the neurons identified as salient by each method and measures their ability to suppress a target concept while minimally affecting auxiliary concepts. Table 5 in Appendix C provides the results for this experiment. Notably, all evaluated saliency methods exhibit degradation in auxiliary concepts when salient neurons for a target concept are masked. One explanation for such deterioration in auxiliary concepts is due to the *polysemantic* neurons. That is, if individual neurons encode multiple concepts, interventions targeting a specific concept can inadvertently disrupt other concepts co-represented within the same neurons.

While any saliency method can be used to identify influential neurons, *we adopt max activation ranking throughout this work because it provides the strongest targeted suppression* as compared to other evaluated methods while exhibiting comparable degradation in auxiliary concepts.
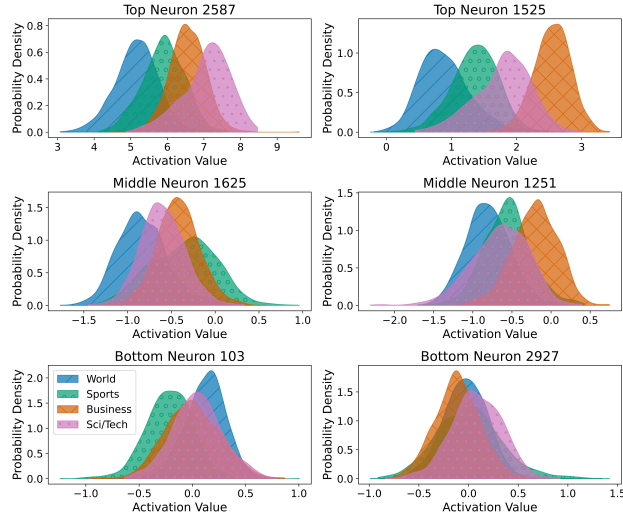
Figure 3: Neuronal activation patterns of six neurons in the Llama model on *AG-News* . Top: neurons sampled from the highest-activating group; middle: from the mid-ranked; bottom: from the lowest-activating group.

3 Polysemanticity

Recent work in polysemanticity (Lecomte et al., 2024; Marshall & Kirchner, 2024) shows that individual neurons learn multiple seemingly unrelated concepts. Polysemanticity often arises when models must represent more features than their capacity allows or due to specific training paradigms (Anthropic, 2023). Training methods like subword tokenization, designed to reduce vocabulary size and model complexity, lead to context-dependent token splits, causing activations to encode multiple meanings (Sennrich et al., 2016; Elhage et al., 2022; Meng et al., 2022). Additionally, Lecomte et al. (2024) show that even with sufficient capacity, weight initializations can induce polysemanticity by placing neurons near multiple conceptual regions. Irrespective of its cause, the polysemanticity of neurons, including salient neurons that encode multiple concepts, challenges the discrete neuron-to-concept attribution paradigm, which maps a concept to an entire neuron.

Polysemanticity in Salient Neurons. To study polysemanticity in salient neurons, we consider a neuron to be polysemantic if it appears salient for more than one concept. We calculate the overlap between the top 30% salient neurons (i.e., max activations) in a model across different classes of diverse datasets. Figure 2 presents the results on GPT-2 model using five different datasets. We observe a considerable overlap in salient neurons between concepts (i.e., classes). For instance, in the case of a two-class dataset, IMDB, the overlap in salient neurons is more than 60%, showing a high degree of polysemanticity.

4 Neuronal Activation Patterns

The prevalence of polysemanticity in salient neurons raises a natural follow-up question: *how do multiple concepts manifest within the activations of a single neuron?* To investigate this question, we analyze the activation patterns of salient neurons extracted via maximal activation, including those that exhibit polysemantic behavior. Specifically, we examine neuron activations conditioned on individual concepts across multiple datasets. Similar to Gurnee et al. (2024), we observe that neuronal activations form Gaussian-like distributions. Importantly, our findings further indicate that for a given salient neuron, *activations associated with different concepts form distinct Gaussian-like distributions with limited overlap*, suggesting that concepts tend to occupy characteristic regions within a neuron's activation spectrum. In the following, we present qualitative and quantitative analyses of the concept-conditioned activation patterns.

Table 1: Skewness, kurtosis, and Kolmogorov-Smirnov stest results across various datasets for Llama model.

Dataset	Skewness	Kurtosis	KS-Test
stanfordnlp/imdb	0.0003	3.9251	0.9995
fancyzhx/dbpedia_14	0.0068	3.9916	0.9133
dair-ai/emotion	0.0000	3.1609	0.9988
fancyzhx/ag_news	-0.0020	3.4079	0.9995
stanfordnlp/sst2	-0.0034	3.5890	0.9993

4.1 Qualitative Analysis

To visually demonstrate that neuron activations for a concept c follow a Gaussian-like distribution, we extract model activations as described in § 2. Using saliency ranking r_c for the dataset, we examine neurons from different ranking positions in the Llama model on the AG-News dataset. In Figures 3, we visualize these distributions using Kernel Density Estimation (KDE).

It reveals that the activations are Gaussian-like for different concepts, where salient neurons demonstrate distinct activation patterns with limited overlap, middle-ranked neurons show a higher degree of overlap than the top ones, whereas non-salient neurons (bottom two) exhibit the highest overlap in activation distributions. Additional analysis for different types of polysemantic neurons for the GPT-2 model is provided in Appendix D. For example figure 6 in Appendix D visualizes two distinct types of polysemantic neurons. One maintains partially separable activation patterns despite being polysemantic; the other exhibits completely overlapping activations. Figure 7 in Appendix D, we present a broader analysis of 7 neurons from the polysemantic subset for 14 total classes. We observe that most polysemantic neurons exhibit limited overlap between concepts at the distributional level with distinct means.

Text Analysis. We complement the activation analysis with a qualitative text analysis that examines representative samples associated with different regions of concept-conditioned activation distributions. Specifically, for selected neurons showcased in Figure 3, we analyze samples drawn from the lower boundary, mean, and upper boundary of their activation distributions. Table 2 presents representative examples for neurons 1525 and 2587, which are predominantly associated with *Sci/Tech* and *Business* concepts, respectively. For neuron 1525, samples near the mean of the distribution focus on core *Sci/Tech* terminology, while samples near the upper boundary reflect a mix of *Sci/Tech* and *Business* concepts (e.g., "subscription plans"). In contrast, samples near the lower boundary tend to blend *Sci/Tech*, *Sports* (e.g., "marathon"), and *World* themes. A similar pattern is observed for neuron 2587: samples near the mean focus on core *Business* topics, transition toward *World*-related content near the lower boundary (e.g., "Asia headquarters"), and shift toward *Sci/Tech* concepts near the upper boundary (e.g., "database demand"). These examples indicate that *changes in activation magnitude correspond to semantic transitions*, providing qualitative evidence that different concepts occupy characteristic regions within a neuron's activation spectrum. Additional details of the text analysis are provided in Appendix E.

4.2 Quantitative Analysis

For each neuron, we collect activation values over samples associated with concept $c \in C$ and compute summary statistics that capture deviations from normality. Specifically, we measure skewness and kurtosis (Joanes & Gill, 1998), and assess goodness-of-fit to a normal distribution using the Kolmogorov–Smirnov (KS) test (Massey Jr, 1951). Table 1 presents the results across all neurons in Llama model. The average skewness is close to 0 across all datasets, indicating strong symmetry (ideal normal distribution: 0), and the average kurtosis is close to 3, nearly identical to the expected value for a normal distribution (3.0).

To assess normality, while accounting for practical significance, we employ the KS test with an effect size threshold of 10%. This approach tests whether the distribution remains within a reasonable bound of normality, rather than testing for perfect normality, which is overly strict for real-world data. For each neuron, we normalize the activations to zero mean and unit variance, then compute the KS statistic against a standard normal distribution. The KS statistic represents the maximum absolute difference between the empirical and theoretical cumulative distribution functions. Using a threshold of 0.1 (allowing a maximum

Table 2: Semantic concepts are highlighted by class color: **World (Blue)**, **Sports (Green)**, **Business (Orange)**, and **Sci/Tech (Purple)**. For each neuron, examples are shown from the lower boundary, mean, and upper boundary of the neuron activations, illustrating how semantic content varies across activation magnitudes. The table shows shortened texts; full reference texts are provided in Appendix **??**.

Neuron	Point	Boundary Affinity	Representative Examples (Concepts Highlighted)
1525	Lower Boundary	**World / Sports**	"**Gene Tweaking** Turns... **Racers**...**single gene** turned...**marathon racers** that could **run for hours**." "**Insecure elections**...**marching**...**soldiers overseas**...ballots via **e-mail**...**PDF**...**Defense Department**." "**IBM**'s **supercomputer** breaks **world's fastest**...**NEC**'s Earth Simulator...based at **Yokohama, Japan**."
	Mean	**Sci/Tech**	"...**powerful chip**...**microprocessor**...appearing in **video game consoles** and **high-definition T-Vs**." "**AMD**...**Dual-Core Opteron**...faster than **single-core chips**...fit in existing **server designs**." "Arm reveals **multimedia**...**Microprocessor** designer...**multimedia technology** for **mobile electronics**."
	Upper Boundary	**Business**	"iPass..**Flat-Rate Pricing Plans** for US **Wi-Fi Hotspot**...**subscription plans** for use..**Wi-Fi connectivity**." "NTT DoCoMo...**Tokyo Stock Exchange**...**procuring mobile phone handsets** made by **Motorola Inc**." "Omnipod...**companies of all sizes**...enhancements...**Web-based client**...a **persistent-chat feature**."
2587	Lower Boundary	**World / Sports**	"**Put Me in, Coach!**. Coach joins the **S&P 500**...leather in the weather as the **global stock market** reacts." "The **London Stock Exchange** plans...**Asia headquarters** in **Hong Kong**...eyeing **stock listings abroad**." "**Halliburton** closes higher... **Army**'s decision...**shares closed higher**...**contract** to supply **US troops in Iraq**."
	Mean	**Business**	"UBS...**capital markets unit** for **$265 million in cash**, strengthening...**brokerage business**" "**Applied Materials**... **shares** were off... in **trading**... wavered around **break-even**... **results** were announced." "Brown-Forman...**jump in earnings** as **aggressive marketing** boosted **sales of premium spirits**."
	Upper Boundary	**Sci/Tech**	"Arm to pay...**$910m in cash and shares** for...**transistor-level designer for systems-on-a-chip**" "**Oracle sales rise** on **database demand**... focus... obtaining **CRM and ERP software**..." "The...**information technology**...**productivity gains**, **business software, and telecommunications** ..."

10% deviation from normal), we find that close to 100% of the neurons exhibit practically normal distributions. The combination of near-ideal skewness and kurtosis values, visual confirmation through KDEs, and our effect size-based KS tests provides strong evidence that the concept-conditioned activations follow approximately normal distributions.

Additionally, we report layer-wise quantitative statistics for the GPT-2 model in Appendix F.1. As layer depth increases, kurtosis steadily converges toward the Gaussian reference value of 3.0, skewness remains near zero, and the 10% practical-normality score stays close to 1 across the network. A qualitative, layer-wise analysis in Appendix F.2 shows that while concept-conditioned Gaussian-like activation patterns are present across all layers, early layers exhibit substantial overlap between concepts. Beginning as early as layers 5–6, distinct concept-specific Gaussians emerge and become progressively more separable in later layers, transitioning toward class-specific semantics.

5 NeuronLens

Given that neuronal activations exhibit approximately Gaussian-like, concept-conditioned distributions with distinct means, we can interpret and intervene on neurons more precisely by operating on activation ranges

rather than attributing entire neurons to individual concepts. This perspective applies regardless of whether a neuron is monosemantic or polysemantic, as it leverages a neuron's activation spectrum. To operationalize this idea, we propose NeuronLens that enables range-based attribution and targeted intervention on neurons.

5.1 Range-based Attribution

NeuronLens computes attribution ranges with respect to a concept using means and standard deviations of the neuronal activations. Specifically, given H_c^l that denotes the set of hidden state vector $\mathbf{h}^l(x_c)$ at layer l for all training samples x_c associated with concept $c \in C$, it can calculate the empirical average $\mu \in \mathbb{R}$ and standard deviation $\sigma \geq 0$ of the activation values of the j-th neuron h_j^l for all samples associated with the concept c as:

$$\mu = \frac{1}{|H_c^l|} \sum_{\mathbf{h}^l \in H_c^l} h_j^l, \sigma = \sqrt{\frac{1}{|H_c^l|} \sum_{\mathbf{h}^l \in H_c^l} (h_j^l - \mu)^2}.$$

Then, it can attribute the activation range of the j-th neuron at layer l to the concept c as:

$$\mathrm{AR}(l, j, c) = [\mu - \tau \times \sigma, \ \mu + \tau \times \sigma],$$

where $\tau > 0$ is a hyperparameter which controls the attribution scope. Intuitively, a smaller τ yields a narrower, conservative range, while a larger τ expands coverage at the risk of including less concept-specific activations. *AR* is defined as attribution range associated with a given concept c.

5.2 Causal Validation

Causal validation is among the most faithful ways to assess attribution correctness (Feder et al., 2021; Vig et al., 2020), as it directly tests whether intervening on the attributed component produces the intended behavioral change, while measuring unintended side effects. Following prior intervention-based validation (Dalvi et al., 2019b; Dai et al., 2022; Dalvi et al., 2019c; Morcos et al., 2018), we utilize concept erasure as a diagnostic intervention to determine the causal effect of identified ranges within neurons for a given concept. The core idea is that if an attribution is salient to a concept, eliminating it should result in the degradation of model's performance on that concept while causing minimal disruption to other concepts. Formally, given a concept-learning model M that maps any input instance x (or part of an instance) to a concept $M(x) = c \in C$, an ideal intervened model M'_{ideal} after erasing a target concept $c \in C$ should satisfy the following property:

$$M'_{\mathrm{ideal}}(x) = \begin{cases} \neq M(x) & \text{if } M(x) = c, \\ = M(x) & \text{if } M(x) \neq c. \end{cases} \tag{1}$$

NeuronLens enables precise manipulation of target concepts via identified activation ranges in contrast to the manipulation and ablation of complete neuron activations. Specifically:

$$h_j^l(x) = \begin{cases} \phi(x) & \text{if } h_j^l(x) \in \mathrm{AR}(l, j, c) \\ h_j^l(x) & \text{otherwise} \end{cases} \tag{2}$$

where $\phi(.)$ is a user-specified range-gated activation operator applied only when $h_j^l(x) \in \mathrm{AR}(l, j, c)$. In general, ϕ can be any function, instantiated for causal intervention (e.g., clamping, zeroing, scaling) or for explanation/attribution (e.g., masking or tagging activations). For concept erasure, the gated function $\phi(.)$ zeroes out which is in line with Dai et al. (2022); Antverg & Belinkov (2022). Some studies have argued that zeroing out neurons is an overly aggressive intervention that can lead to catastrophic degradation in model performance. In Appendix G, we compare alternative activation interventions, including the *dampening* method (Suau et al., 2024) and *mean replacement* (Suau et al., 2021). Erasure experiments in the main text ablating a specific range of neuronal activation are referred as range-based masking, whereas ablating the complete neurons is referred as neuron masking.

Table 3: Evaluation of selected models on AG-News, Emotions, and DBPedia-14 datasets using activation range and neuron masking techniques. Performance metrics are calculated using class level 10% trimmed means at the class level. Metrics are detailed in § 5.3. For *GPT-2* and *Bert* 50% and for *Llama-3.2-3B* 30% neurons are selected.

Model	Dataset	Base Values				Neuron Masking				Activation Range Masking (ARM)			
		Acc	Conf	CAcc	CConf	Acc	Conf	CAcc	CConf	Acc	Conf	CAcc	CConf
	AG-NEWS	0.948	0.929	0.948	0.929	-0.271	-0.590	0.012	-0.074	-0.261	-0.590	**0.013**	**-0.009**
	Emotions	0.894	0.834	0.917	0.876	-0.291	-0.633	0.013	-0.265	-0.279	-0.635	**0.014**	**-0.069**
BERT	DBPedia-14	0.992	0.991	0.990	0.989	-0.028	-0.786	0.000	-0.017	-0.015	-0.766	0.000	**-0.000**
	AG-NEWS	0.945	0.933	0.945	0.933	-0.871	-0.877	-0.155	**-0.163**	-0.849	-0.862	**-0.063**	-0.223
	Emotions	0.905	0.892	0.930	0.919	-0.735	-0.738	-0.103	-0.103	-0.737	-0.739	**-0.044**	**-0.046**
GPT-2	DBPedia-14	0.993	0.990	0.990	0.988	-0.810	-0.845	-0.154	-0.177	-0.782	-0.825	**-0.015**	**-0.031**
	AG-NEWS	1.000	0.744	1.000	0.744	-0.934	-0.725	-0.660	-0.572	-0.935	-0.725	**-0.484**	**-0.454**
	Emotions	0.815	0.472	0.823	0.477	-0.795	-0.470	-0.696	-0.429	-0.797	-0.469	**-0.594**	**-0.404**
Llama	DBPedia-14	1.000	0.533	1.000	0.563	-0.992	-0.528	-0.912	-0.445	-0.986	-0.527	**-0.663**	**-0.354**

Table 4: Evaluation of latent capabilities of Llama model after applying neuron and range-based masking. Base PPL = 7.007; Base MMLU = 0.53.

Dataset	Neuron Masking		ARM	
	Perplexity	MMLU	Perplexity	MMLU
AG-NEWS	12.757	0.510	8.022	0.533
Emotions	11.630	0.526	8.063	0.526
DBPedia-14	12.230	0.507	7.903	0.535

5.3 Experimental Setup

We incorporate our intervention at the penultimate layer. Ablation for layer selection is provided in the Appendix F. The training details for the fine-tuned models are provided in Appendix H.

Metrics. We causally validate the attribution using two metrics: prediction accuracy and the model's predictive probability as a proxy for confidence score. First, baseline measurements of both accuracy and confidence for all concepts C without any intervention (unmodified model) are established. Post-intervention measurements are recorded for the target concept c and auxiliary concepts (other concepts in the dataset) c'. The effectiveness and precision of attribution are assessed through two key metrics: (1) the performance degradation for concept c, and (2) the extent of unintended impact on auxiliary concepts c'. Throughout our analysis, we denote the accuracy and confidence metrics for concept c as **Acc** and **Conf** respectively, while corresponding measurements for auxiliary concepts c' are represented as **CAcc** and **CConf**. For evaluating the effect of the interventions on LLMs latent capabilities, we utilize **perplexity (PPL)** and zero-shot accuracy on **MMLU**.

Hyperparameter. The value of τ is set to 2.5, assuming a fully Gaussian distribution. This threshold corresponds to a coverage of approximately 98.76% of the distribution, providing a slightly conservative bound for range-based interventions. Ablations for varying τ are presented in Appendix I. The results indicate that targeted concept deteriorates up to 2.4-2.7 τ then plateaus, while auxiliary concepts begin to degrade further.

5.4 Results and Analysis

Table 3 presents results for the concept erasure task across five benchmark datasets (Class-wise detailed results are provided in Appendix J), demonstrating the effectiveness of range-based masking compared to traditional neuron masking. Results in Table 3 show that multi-class classification tasks with fine-grained labels, such as AG-News, Emotions, and DBPedia-14, exhibit more pronounced effects under intervention. Range-based masking results in significant degradation of primary task performance while preserving auxiliary concept accuracy. This is particularly evident in results for AG-News. On binary classification tasks (IMDB, SST2) provided in appendix J (Table 17 and 16), both masking approaches show moderate performance drops in targeted concepts. This suggests higher redundancy for coarser binary concepts.
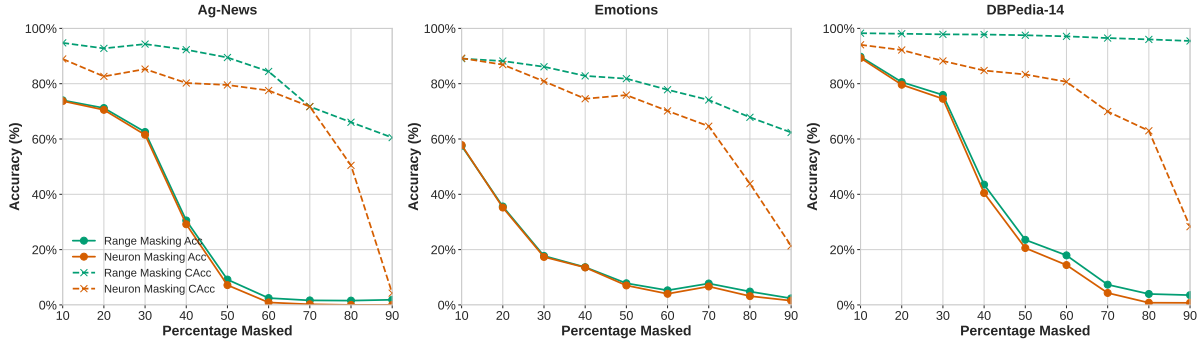
Figure 4: Accuracy on the GPT-2 model as a function of the percentage of masked neurons, comparing activation range-based masking (green) and neuron-level masking (orange).

GPT-2, despite being fine-tuned but trained in an autoregressive manner, shows substantially higher vulnerability with major drops in AG-NEWS ($\Delta_{acc} = -0.849$) and DBPedia-14 ($\Delta_{acc} = -0.782$). This increased sensitivity may be attributed to its autoregressive training objective, which potentially leads to more sequential and less redundant concept encodings. The Llama-3.2-3B model, evaluated in a few-shot setting without task-specific training, experiences the most severe degradation across all datasets (often exceeding -0.90), suggesting that pre-trained representations without task-specific fine-tuning are more vulnerable to full neuron interventions.

General LLM Capabilities. To ensure that our approach does not compromise general model capabilities, we evaluate the impact of range-based masking on language modeling quality and broad knowledge and reasoning performance using the MLU benchmark. Table 4 presents the comparative performance of neuron masking and activation range masking. Full neuron masking leads to notable increases in perplexity, exceeding 3 points in the best case, whereas range masking results in a maximum increase of only 1.1. In terms of MMLU accuracy, neuron masking consistently reduces performance across all settings, while range masking preserves or improves performance in most cases, with degradation observed in only one instance.

Alternative activation interventions. We also experiment with alternative activation interventions. Details of the alternative approaches are provided in Appendix G. While dampening and mean replacement methods aim to manipulate without moving too far from the original representation, they exhibit limitations when applied to neurons. Specifically, neuron dampening increases perplexity by 2.9–3.7 points and often degrades MMLU accuracy (up to -0.045), whereas range-based dampening confines perplexity increases to 0.5–0.8 points and occasionally improves MMLU (up to +0.035). Similarly, mean replacement leads to substantial degradation when applied to neurons (perplexity increases of 7.4–8.8), while range-based replacement reduces the impact to below 0.7 points.

However, both dampening and mean replacement methods suffer from rigid static suppression or substitution, failing to account for concept-specific activation dynamics. To address this issue, we introduce a novel **adaptive dampening** technique. This method modulates suppression in proportion to each activation's deviation from its class-conditional mean, enabling suppression guided by sampled observations. Adaptive dampening achieves the strongest balance across all metrics: perplexity remains low (0.41–0.61), MMLU is maintained or improved (up to +0.03), and collateral damage to auxiliary concepts is minimized (CAcc drops consistently below -0.3, often under -0.15), outperforming dampening, mean replacement, and zeroing out approaches.

These results demonstrate that precise intervention in specific activation ranges enables substantially more targeted concept manipulation while preserving auxiliary concepts, highlighting how conceptual information is encoded within specific activation patterns rather than isolated to individual neurons, underscoring the importance of activation ranges in capturing neuron-concept relationships.

Percentage Masking Effect. As the masking rate increases, the advantage of range-based masking over the neuron-masking baseline becomes increasingly pronounced. Beyond a critical masking level, the baseline

exhibits a sharp performance collapse, whereas our method avoids this cliff and degrades smoothly all the way to full masking (100%). This arises from two factors: (1) models have a large number of polysemantic neurons, and higher masking rates increase the chance of ablating them, and (2) blocking/manipulating a higher percentage of the model's neurons creates a significant deviation from the original model's behavior. For low-activation neurons with respect to the concept of interest, discrete neuron masking (i.e., completely masking out a neuron) becomes unreliable, as shown in Figure 4, with a steep performance drop after masking 50% of neurons. Notably, our range-based method offers finer-grained attribution, preserving model behavior under extensive masking. The relatively stable results on auxiliary concept when using range-based masking at a high percentage of neurons reduce the need to find an optimum threshold for the number of neurons to ablate, which is critical to neuron masking.

6 Related Work

While we have discussed closely related approaches in § 2, we briefly review additional relevant techniques here. Circuit discovery identifies groups of neurons that jointly encode concepts, providing a structured view of model behavior (Marks et al., 2024; Conmy et al., 2023; Olah et al., 2020). However, extracting circuits is computationally intensive and lacks fine-grained neuron-level attribution. Gradient-based methods attribute predictions to input features by tracking gradients through the network, with integrated gradients (Sundararajan et al., 2017; Dai et al., 2022) being a widely used approach. However, they struggle with polysemanticity, as they do not disentangle overlapping concepts within neurons. Causal analysis methods intervene on internal components to assess their role in encoding concepts. Causal tracing measures the effect of corrupting activations on model performance (Vig et al., 2020; Meng et al., 2022), while causal mediation analysis quantifies information propagation through neurons (Vig et al., 2020). Although effective, these techniques require costly perturbation experiments. Beyond neuron-level analysis, representation-level methods examine hidden states and their relationship to model outputs and concepts (Veldhoen et al., 2016; Tenney et al., 2019; Liu et al., 2019). Sparse probing (Gurnee et al., 2023) compresses hidden representations into sparse, interpretable subspaces. While prior work has advanced interpretability, most methods rely on discrete neuron-to-concept mappings, which fail to account for polysemanticity (Sajjad et al., 2022). Our work extends activation-based approaches by introducing activation ranges as the unit of interpretability, enabling more precise concept attribution and intervention.

7 Conclusion

In this work, we revisited neuron-level interpretability through the lens of polysemanticity and showed that, despite encoding multiple concepts, individual neurons exhibit predictable activation behavior. Through systematic qualitative and quantitative analysis, we demonstrated that concept-conditioned neuron activations form Gaussian-like distributions with limited overlap. Building on this observation, we introduced NeuronLens, a range-based framework that attributes concepts to activation ranges rather than entire neurons. NeuronLens enables more precise concept manipulation by selectively intervening within these ranges while substantially reducing unintended interference with auxiliary concepts. Our causal evaluations show that range-based masking consistently outperforms full neuron masking and preserves general model capabilities, including broad knowledge and reasoning performance measured by MMLU, as well as language modeling quality.

References

Anthropic. A toy model of double descent from sparsely-gated routing. *Transformer Circuits*, 2023. URL https://transformer-circuits.pub/2023/toy-double-descent/index.html.

Omer Antverg and Yonatan Belinkov. On the pitfalls of analyzing individual neurons in language models. In *The Tenth International Conference on Learning Representations, ICLR 2022, Virtual Event, April 25-29, 2022*. OpenReview.net, 2022. URL https://openreview.net/forum?id=8uzOEWPQIMu.

Arthur Conmy, Augustine Mavor-Parker, Aengus Lynch, Stefan Heimersheim, and Adrià Garriga-Alonso. Towards automated circuit discovery for mechanistic interpretability. *Advances in Neural Information Processing Systems*, 36:16318–16352, 2023.

Damai Dai, Li Dong, Yaru Hao, Zhifang Sui, Baobao Chang, and Furu Wei. Knowledge neurons in pretrained transformers. In Smaranda Muresan, Preslav Nakov, and Aline Villavicencio (eds.), *Proceedings of the 60th Annual Meeting of the Association for Computational Linguistics (Volume 1: Long Papers)*, pp. 8493–8502, Dublin, Ireland, May 2022. Association for Computational Linguistics. doi: 10.18653/v1/2022.acl-long.581. URL https://aclanthology.org/2022.acl-long.581/.

Fahim Dalvi, Nadir Durrani, Hassan Sajjad, Yonatan Belinkov, Anthony Bau, and James R. Glass. What is one grain of sand in the desert? analyzing individual neurons in deep NLP models. In *The Thirty-Third AAAI Conference on Artificial Intelligence, AAAI 2019, The Thirty-First Innovative Applications of Artificial Intelligence Conference, IAAI 2019, The Ninth AAAI Symposium on Educational Advances in Artificial Intelligence, EAAI 2019, Honolulu, Hawaii, USA, January 27 - February 1, 2019*, pp. 6309–6317. AAAI Press, 2019a. doi: 10.1609/AAAI.V33I01.33016309. URL https://doi.org/10.1609/aaai.v33i01.33016309.

Fahim Dalvi, Nadir Durrani, Hassan Sajjad, Yonatan Belinkov, D. Anthony Bau, and James Glass. What is one grain of sand in the desert? analyzing individual neurons in deep nlp models. In *Proceedings of the AAAI Conference on Artificial Intelligence (AAAI)*, March 2019b.

Fahim Dalvi, Avery Nortonsmith, D Anthony Bau, Yonatan Belinkov, Hassan Sajjad, Nadir Durrani, and James Glass. Neurox: A toolkit for analyzing individual neurons in neural networks. *Proceedings of the AAAI Conference on Artificial Intelligence (AAAI)*, 2019c.

Jacob Devlin, Ming-Wei Chang, Kenton Lee, and Kristina Toutanova. Bert: Pre-training of deep bidirectional transformers for language understanding, 2019. URL https://arxiv.org/abs/1810.04805.

Nelson Elhage et al. Superposition, memorization, and double descent. *Transformer Circuits*, 2022.

Amir Feder, Nadav Oved, Uri Shalit, and Roi Reichart. Causalm: Causal model explanation through counterfactual language models. *Computational Linguistics*, 47(2):333–386, 2021.

Alex Foote, Neel Nanda, Esben Kran, Ionnis Konstas, and Fazl Barez. N2g: A scalable approach for quantifying interpretable neuron representations in large language models. *arXiv preprint arXiv:2304.12918*, 2023.

Wikimedia Foundation. Wikimedia downloads. URL https://dumps.wikimedia.org.

Jonathan Frankle and Michael Carbin. The lottery ticket hypothesis: Finding sparse, trainable neural networks, 2019. URL https://arxiv.org/abs/1803.03635.

Aaron Grattafiori. The llama 3 herd of models, 2024. URL https://arxiv.org/abs/2407.21783.

Wes Gurnee, Neel Nanda, Matthew Pauly, Katherine Harvey, Dmitrii Troitskii, and Dimitris Bertsimas. Finding neurons in a haystack: Case studies with sparse probing, 2023. URL https://arxiv.org/abs/2305.01610.

Wes Gurnee, Theo Horsley, Zifan Carl Guo, Tara Rezaei Kheirkhah, Qinyi Sun, Will Hathaway, Neel Nanda, and Dimitris Bertsimas. Universal neurons in gpt2 language models. *arXiv preprint arXiv:2401.12181*, 2024.

Dan Hendrycks, Collin Burns, Steven Basart, Andy Zou, Mantas Mazeika, Dawn Song, and Jacob Steinhardt. Measuring massive multitask language understanding. In *9th International Conference on Learning Representations, ICLR 2021, Virtual Event, Austria, May 3-7, 2021*. OpenReview.net, 2021. URL https://openreview.net/forum?id=d7KBjmI3GmQ.

Derrick N Joanes and Christine A Gill. Comparing measures of sample skewness and kurtosis. *Journal of the Royal Statistical Society: Series D (The Statistician)*, 47(1):183–189, 1998.

Victor Lecomte, Kushal Thaman, Rylan Schaeffer, Naomi Bashkansky, Trevor Chow, and Sanmi Koyejo. What causes polysemanticity? an alternative origin story of mixed selectivity from incidental causes. In *ICLR 2024 Workshop on Representational Alignment*, 2024.

Nelson F. Liu, Matt Gardner, Yonatan Belinkov, Matthew E. Peters, and Noah A. Smith. Linguistic knowledge and transferability of contextual representations. In Jill Burstein, Christy Doran, and Thamar Solorio (eds.), *Proceedings of the 2019 Conference of the North American Chapter of the Association for Computational Linguistics: Human Language Technologies, Volume 1 (Long and Short Papers)*, pp. 1073–1094, Minneapolis, Minnesota, June 2019. Association for Computational Linguistics. doi: 10.18653/v1/N19-1112. URL https://aclanthology.org/N19-1112/.

Andrew Maas, Raymond E Daly, Peter T Pham, Dan Huang, Andrew Y Ng, and Christopher Potts. Learning word vectors for sentiment analysis. In *Proceedings of the 49th annual meeting of the association for computational linguistics: Human language technologies*, pp. 142–150, 2011.

Samuel Marks, Can Rager, Eric J. Michaud, Yonatan Belinkov, David Bau, and Aaron Mueller. Sparse feature circuits: Discovering and editing interpretable causal graphs in language models. *CoRR*, abs/2403.19647, 2024. doi: 10.48550/ARXIV.2403.19647. URL https://doi.org/10.48550/arXiv.2403.19647.

Simon C. Marshall and Jan H. Kirchner. Understanding polysemanticity in neural networks through coding theory, 2024. URL https://arxiv.org/abs/2401.17975.

Frank J Massey Jr. The kolmogorov-smirnov test for goodness of fit. *Journal of the American statistical Association*, 46(253):68–78, 1951.

Kevin Meng, David Bau, Alex Andonian, and Yonatan Belinkov. Locating and editing factual associations in GPT. *Advances in Neural Information Processing Systems*, 2022.

Ari S. Morcos, David G. T. Barrett, Neil C. Rabinowitz, and Matthew Botvinick. On the importance of single directions for generalization, 2018. URL https://arxiv.org/abs/1803.06959.

Chris Olah, Nick Cammarata, Ludwig Schubert, Gabriel Goh, Michael Petrov, and Shan Carter. Zoom in: An introduction to circuits. *Distill*, 5(3):e00024–001, 2020.

Alec Radford, Jeffrey Wu, Rewon Child, David Luan, Dario Amodei, and Ilya Sutskever. Language models are unsupervised multitask learners. *OpenAI Blog*, 1(8):9, 2019.

Hassan Sajjad, Nadir Durrani, and Fahim Dalvi. Neuron-level interpretation of deep nlp models: A survey, 2022. URL https://arxiv.org/abs/2108.13138.

Victor Sanh, Lysandre Debut, Julien Chaumond, and Thomas Wolf. Distilbert, a distilled version of bert: smaller, faster, cheaper and lighter, 2020. URL https://arxiv.org/abs/1910.01108.

Elvis Saravia, Hsien-Chi Toby Liu, Yen-Hao Huang, Junlin Wu, and Yi-Shin Chen. CARER: Contextualized affect representations for emotion recognition. In *Proceedings of the 2018 Conference on Empirical Methods in Natural Language Processing*, pp. 3687–3697, Brussels, Belgium, October-November 2018. Association for Computational Linguistics. doi: 10.18653/v1/D18-1404. URL https://www.aclweb.org/anthology/D18-1404.

Rico Sennrich, Barry Haddow, and Alexandra Birch. Neural machine translation of rare words with subword units. *Proceedings of the 54th Annual Meeting of the Association for Computational Linguistics*, 2016.

Richard Socher, Alex Perelygin, Jean Wu, Jason Chuang, Christopher D Manning, Andrew Y Ng, and Christopher Potts. Recursive deep models for semantic compositionality over a sentiment treebank. In *Proceedings of the 2013 conference on empirical methods in natural language processing*, pp. 1631–1642, 2013.

Xavier Suau, Luca Zappella, and Nicholas Apostoloff. Self-conditioning pre-trained language models. *arXiv preprint arXiv:2110.02802*, 2021.

Xavier Suau, Pieter Delobelle, Katherine Metcalf, Armand Joulin, Nicholas Apostoloff, Luca Zappella, and Pau Rodríguez. Whispering experts: Neural interventions for toxicity mitigation in language models. *arXiv preprint arXiv:2407.12824*, 2024.

Mukund Sundararajan, Ankur Taly, and Qiqi Yan. Axiomatic attribution for deep networks, 2017. URL https://arxiv.org/abs/1703.01365.

Ian Tenney, Dipanjan Das, and Ellie Pavlick. BERT rediscovers the classical NLP pipeline. In *Proceedings of the 57th Annual Meeting of the Association for Computational Linguistics*, pp. 4593–4601, Florence, Italy, July 2019. Association for Computational Linguistics. doi: 10.18653/v1/P19-1452. URL https://www.aclweb.org/anthology/P19-1452.

Sara Veldhoen, Dieuwke Hupkes, and Willem Zuidema. Diagnostic classifiers: Revealing how neural networks process hierarchical structure. In *Pre-Proceedings of the Workshop on Cognitive Computation: Integrating Neural and Symbolic Approaches (CoCo @ NIPS 2016)*, 2016.

Jesse Vig, Sebastian Gehrmann, Yonatan Belinkov, Sharon Qian, Daniel Nevo, Yaron Singer, and Stuart Shieber. Investigating gender bias in language models using causal mediation analysis. *Advances in neural information processing systems*, 33:12388–12401, 2020.

Elena Voita, Javier Ferrando, and Christoforos Nalmpantis. Neurons in large language models: Dead, n-gram, positional. *arXiv preprint arXiv:2309.04827*, 2023.

Xiang Zhang, Junbo Zhao, and Yann LeCun. Character-level convolutional networks for text classification. In C. Cortes, N. Lawrence, D. Lee, M. Sugiyama, and R. Garnett (eds.), *Advances in Neural Information Processing Systems*, volume 28. Curran Associates, Inc., 2015. URL https://proceedings.neurips.cc/paper_files/paper/2015/file/250cf8b51c773f3f8dc8b4be867a9a02-Paper.pdf.

A Limitations

While NeuronLens can disentangle polysemanticity to a degree using identified Gaussian-like distributions, it is unable to completely disentangle concepts encoded in the polysemantic neurons, as concept-specific activation distributions still partially overlap. We also present results primarily from the penultimate layer, and not the intermediate or earlier layers; however, we provide ablations and rationale for this choice in Appendix F

B Impact Statement

This work advances neural network interpretability by providing a fine-grained understanding of concept encoding in language models. The proposed NeuronLens framework enables precise control of model behavior, benefiting research in model safety and reliability. While this improved understanding could potentially be misused, the work's theoretical nature and focus on interpretability methods makes immediate harmful applications unlikely.

C Details of Saliency Methods

Max Activations (Frankle & Carbin, 2019). Max activations extract high neural activations as a saliency ranking metric relying upon the rationale that maximally activating neurons are salient as these neurons play a critical role in controlling the model's output, highlighting their importance for a concept c. To identify them, the column-wise mean of absolute neuronal activations in H_c^l, H_c^l is defined in §2.3, is computed, given that high negative activations also carry significant signals (Voita et al., 2023). The magnitude of the means is then considered as a ranking for concept c.

Probe Analysis (Dalvi et al., 2019b). Probe analysis trains a linear classifier on the hidden representations H_c^l to distinguish between concepts. The learned model weights are then utilized as a saliency ranking. This process involves learning a weight matrix $W \in \mathbb{R}^{d \times |c|}$, where d is the hidden dimension and $|c|$ is the number of concept classes. The absolute weight values of each row in the weight matrix are used as a ranking for the importance of each neuron for a given concept. To prevent the emergence of redundant solutions characterized by minimal variations in the weights, the probe is trained using the elastic regularization technique.

Probeless (Antverg & Belinkov, 2022). Probeless examines individual neurons, without the need for auxiliary classifiers, using the element-wise difference between mean vectors. The element-wise difference between mean vectors is computed as $r = \sum_{c,c' \in C} |q(c) - q(c')|$, where $r \in \mathbb{R}^d$ and d is the hidden dimension. The final neuron saliency ranking is obtained by sorting r in descending order.

C.1 Causal validation

To causally validate the aforementioned approaches, we apply erasure; the results for this are provided in Table 5. The results show that degradation the target concepts is highest when using max activations.

D Qualitative and Quantitative Analysis on GPT-2

D.1 Qualitative

Following similar experimental setup as used in § 4, here we provide the results for the GPT-2 model. Figure 5 and 6 shows these visualizations. Figure 5 similar to the Llama shows that while the activations are Gaussian-like for different concepts, salient neurons demonstrate distinct activation patterns with limited overlap.

In Figure 6, we identify and visualize two distinct types of polysemantic neurons that appear in the salient sets across all classes, when 5% salient set was selected, in the dataset. The first type, exemplified by neuron 480, maintains partially separable activation patterns despite being polysemantic, suggesting some degree of class-specific behavior. In contrast, the second type, represented by neuron 675, exhibits completely

Table 5: Performance drops relative to Baseline configuration (i.e., unaltered model's performance) for three techniques: Probeless, Probe, and Max. All values show the difference from Base values. Results are for *Emotions* dataset on the GPT-2 model using 30% salient neurons of each method. Metrics are detailed in § 5.3.

Model	Probeless				Probe				Max			
	Acc	Conf	CAcc	CConf	Acc	Conf	CAcc	CConf	Acc	Conf	CAcc	CConf
GPT-2	-0.524	-0.510	-0.086	-0.086	-0.052	-0.036	-0.018	-0.049	**-0.735**	**-0.739**	-0.103	-0.103
Llama	-0.751	-0.292	-0.751	-0.272	-0.177	-0.145	-0.169	-0.096	**-0.805**	**-0.500**	-0.511	-0.399

Table 6: Skewness, kurtosis, and Kolmogorov-Smirnov test results across various datasets. *GPT-2* model

Dataset	Skewness	Kurtosis	KS-Test
stanfordnlp/imdb	0.0014	3.6639	1.0000
fancyzhx/dbpedia__14	-0.0007	3.9360	0.9782
dair-ai/emotion	0.0015	3.0198	0.9446
fancyzhx/ag__news	-0.0013	3.2060	0.9918
stanfordnlp/sst2	-0.0083	3.2038	1.0000

overlapping activation patterns across all classes, making it hard to disentangle. To further investigate this phenomenon, Figure 7 presents a broader analysis of neurons from the polysemantic subset, identified using a 5% saliency threshold (top 5% salient neurons selected for a concept).

D.2 Quantitative

Skewness and Kurtosis results are provided in Table 6. The results are similar to those observed on the Llama model in the main text.
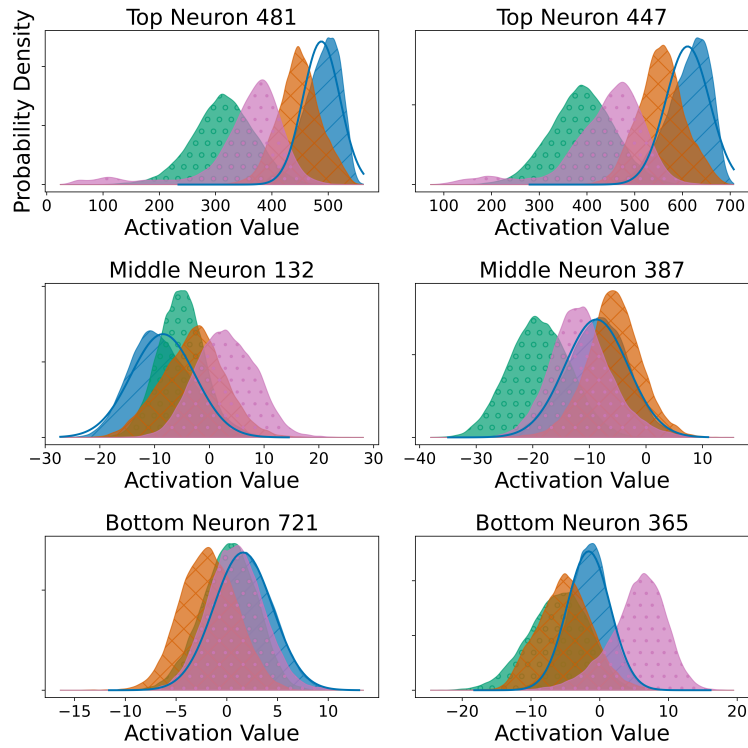
Figure 5: Neuronal Activation Patterns of six neurons on *AG-News* dataset *class 1*. Neurons 418 and 447 are the highest activating neurons, neurons 132 and 387 are middle-ranked neurons, and neurons 721 and 365 are the lowest activating neurons.

Figure 6: Neuronal Activation Patterns comparison of neurons 480 and 675. The plots show class-specific activity patterns with fitted Gaussian curves. Both neurons were part of salient set of all classes when top 5% salient selected on *AG-News* dataset.
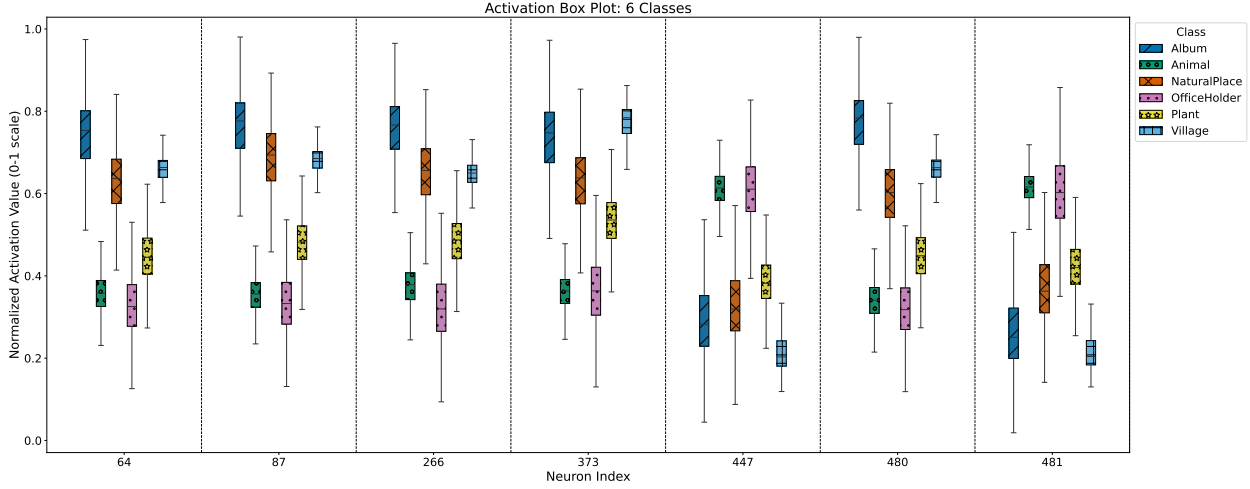
Figure 7: Box plot of neural activation of 7 polysemantic neurons (i.e: neurons in the salient group for all classes, percentage selected: 5% top salient) for 6 randomly selected classes out of 14 classes of *DBPedia-14* dataset.

E Qualitative Text Analysis

After recording the activations and calculating distributions, we calculate the activation range (as defined in § 5.1) for each class in the dataset under consideration. We then extract 10 text examples at each of three points along the computed activation range for each concept: the lower bound (minimum of the activation range), the midpoint (mean of the activation range), and the upper bound (maximum of the activation range).

We then pass these text examples to an LLM judge (Gemini Pro) along with class labels and boundary position information. The LLM judge then extracts the underlying semantics shared in the examples from one of the labels of the dataset, along with highlighted keywords. We present 3 representative examples from each set for one selected class, along with LLM highlighted keywords and semantics in the Table 2, the full relevant texts for the table are provided in Table 7.

F Layer Ablation

F.1 Statistical Results

We analyze concept level activation distributions across all 12 layers of GPT-2, measuring kurtosis (where a value of 3.0 indicates a Gaussian distribution), skewness (where 0 indicates symmetry), and practical normality in Table 8:

These results show that kurtosis values converge toward 3.0 (the Gaussian ideal) as layers progress, skewness values remain near zero across all layers, and practical normality scores are close to 1 across all layers. Importantly, if the activations were not clustered into continuous intervals and were in disconnected islands of activations, these would be reflected in the score for the practical normality and other statistical metrics.

F.2 Qualitative Results

We expanded our visualization approach shown in Figures figs. 8 to 19 in Figure 4) to all layers in the model. The visualizations demonstrate an interesting progression: while all layers exhibit Gaussian-like distributions on the class level, class concepts aren't separated in the activation spectrum Gaussians of the early layers. This aligns with the understanding that lower layers capture more basic features rather than high-level semantic features like class. However, distinct concept-level Gaussian distributions begin forming as early as layers 5-6, becoming increasingly separable in deeper layers.

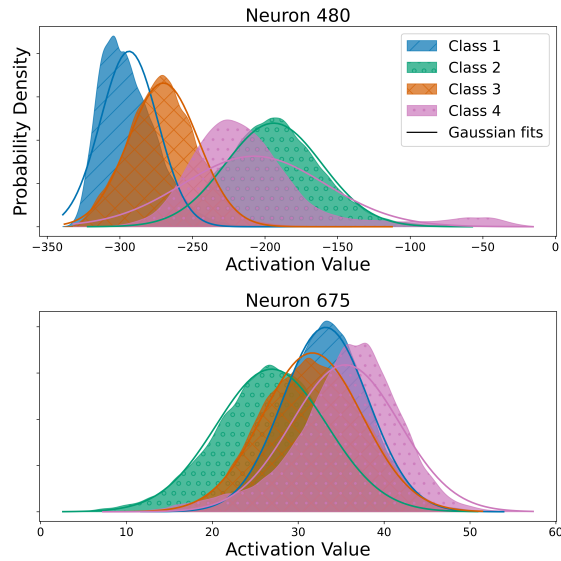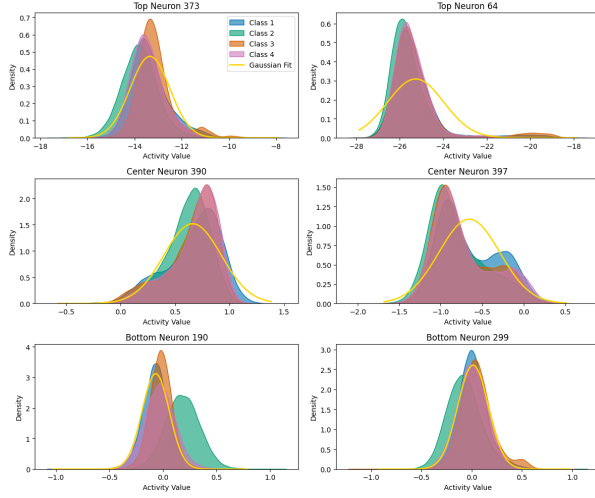Figure 8: Neuronal Activation Patterns of six neurons on *AG-News* dataset. Layer 1
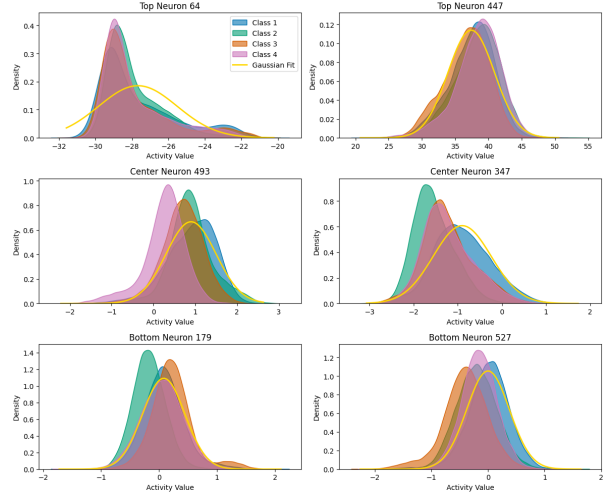
Figure 9: Neuronal Activation Patterns of six neurons on *AG-News* dataset. Layer 2
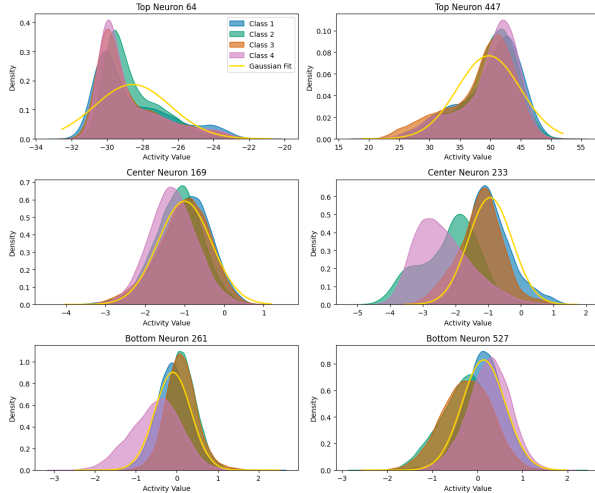
Figure 10: Neuronal Activation Patterns of six neurons on *AG-News* dataset. Layer 3
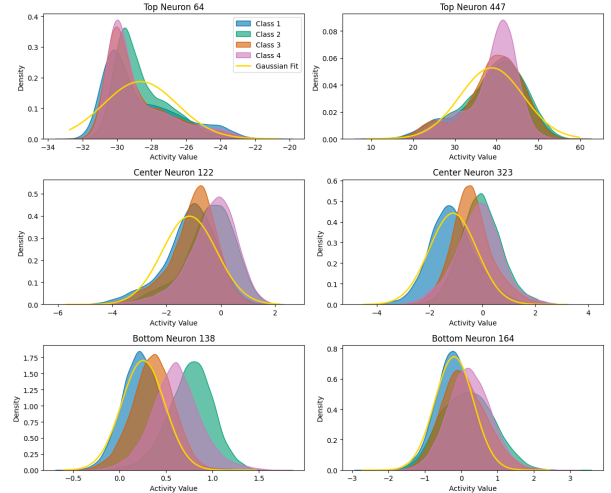
Figure 11: Neuronal Activation Patterns of six neurons on *AG-News* dataset. Layer 4

F.3 Masking Results

In Table 9 and Table 10 we provide results of applying both approaches on all layers of *GPT-2* model on *Emotions* dataset. From the results we can see that: Early layers (1-3) show highly variable and often severe impacts: Layer 1 exhibits minimal effects ($\Delta Acc = -0.113$, $\Delta CAcc = -0.064$), while Layers 2-3 show extreme degradation ($\Delta Acc \approx -0.7$, $\Delta CAcc > -0.5$). Middle layers (4-8) demonstrate inconsistent behavior with high variance in impacts. Layer 12, however, achieves an optimal balance: it maintains substantial primary task impact ($\Delta Acc = -0.571$) while minimizing auxiliary concept interference ($\Delta CAcc = -0.060$). This pattern holds true for both neuron masking and range masking techniques, with range masking showing slightly better preservation of auxiliary concepts ($\Delta CAcc = -0.045$). The mid-range primary task degradation combined with minimal auxiliary impact makes Layer 12 the most suitable for targeted interventions, offering better control and specificity compared to earlier layers.
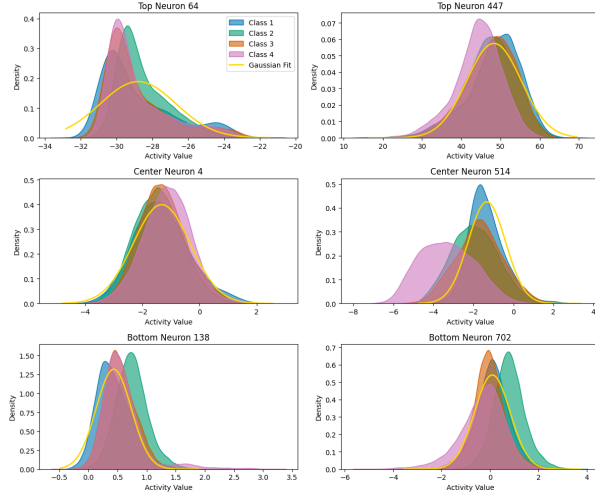
Figure 12: Neuronal Activation Patterns of six neurons on *AG-News* dataset. Layer 5
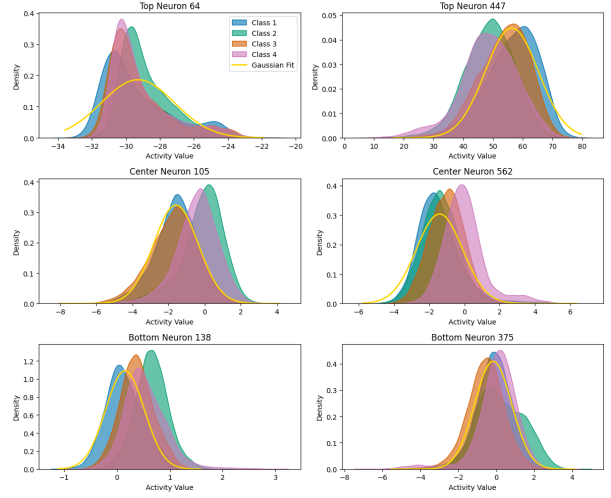
Figure 13: Neuronal Activation Patterns of six neurons on *AG-News* dataset. Layer 6
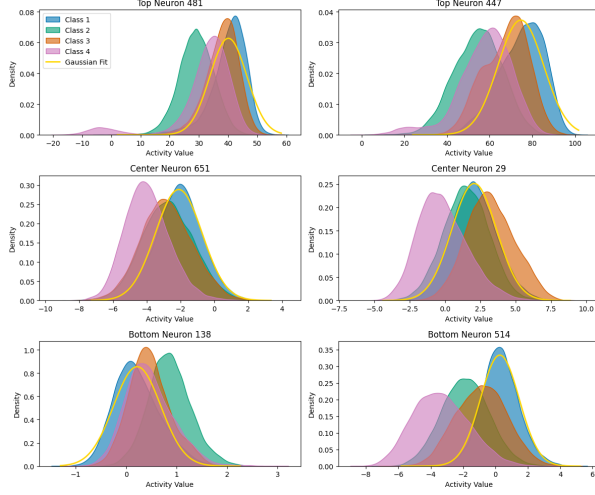
Figure 14: Neuronal Activation Patterns of six neurons on *AG-News* dataset. Layer 7
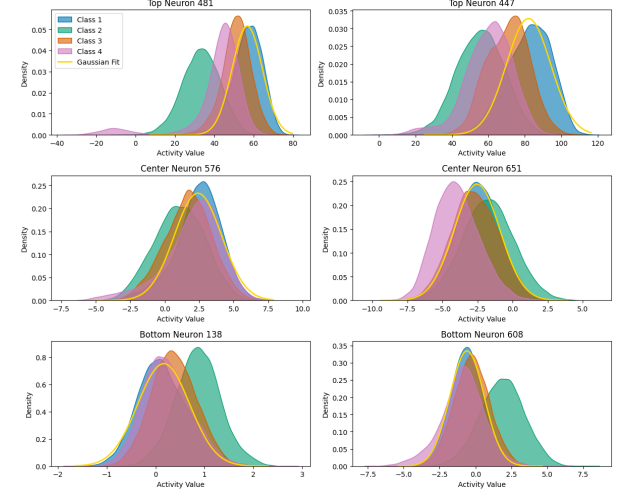
Figure 15: Neuronal Activation Patterns of six neurons on *AG-News* dataset. Layer 8

G   Alternative Activation Interventions

In the main text, we primarily presented results using a "zeroing out" strategy for neuron manipulation. This approach was chosen to compare neuron manipulation against range-based manipulation. However, zeroing out is considered a suboptimal strategy (Suau et al., 2024). The primary concern with standard zeroing-out approaches is that they distort the activation distribution significantly, diverging from that of the original model. However, our range-based method selectively zeroes out only a narrow slice of the activation spectrum, thereby mitigating the adverse effects associated with hard erasure.

In this section, we explore alternative, more optimized strategies for concept removal. We also introduce a novel range-based scaling strategy that has demonstrated superior results.

Below, we explore various activation intervention strategies, comparing traditional neuron-level approaches with the nuanced range-based technique. Our comprehensive evaluation reveals that range-based manipulations consistently outperform neuron interventions across multiple metrics, with significantly less disruption to the model's general capabilities.
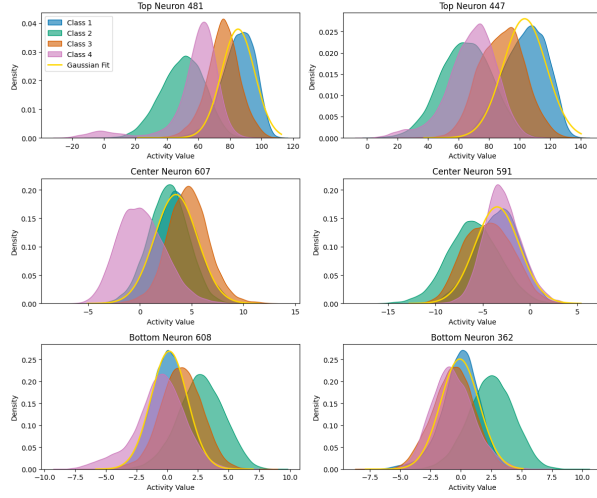
Figure 16: Neuronal Activation Patterns of six neurons on *AG-News* dataset. Layer 9
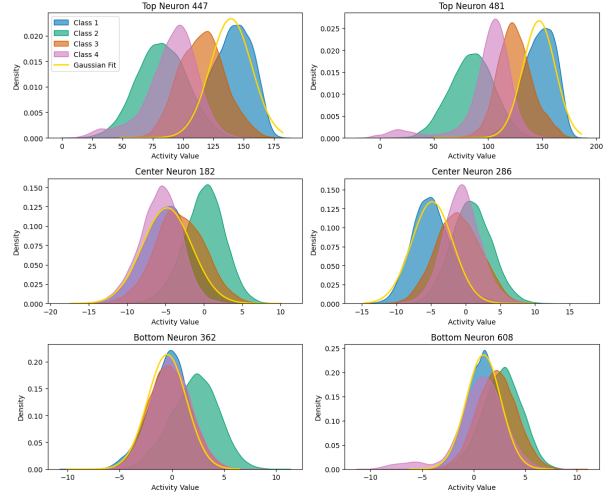
Figure 17: Neuronal Activation Patterns of six neurons on *AG-News* dataset. Layer 10
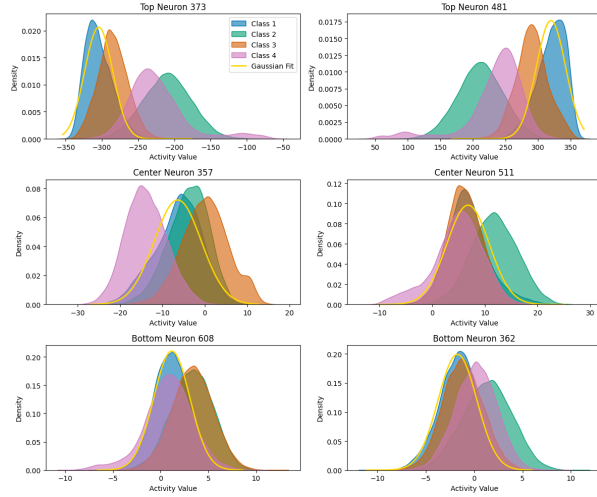
Figure 18: Neuronal Activation Patterns of six neurons on *AG-News* dataset. Layer 11
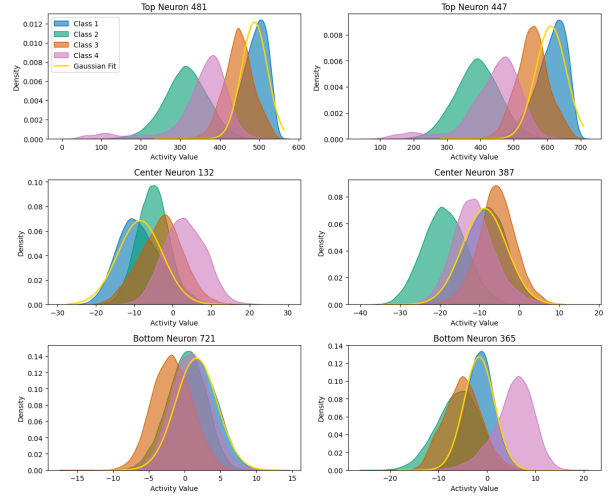
Figure 19: Neuronal Activation Patterns of six neurons on *AG-News* dataset. Layer 12

Among all techniques examined, our novel adaptive dampening approach emerges as the most effective, maintaining targeted concept suppression while minimizing collateral impact on auxiliary concepts and preserving overall language modelling capabilities. This pattern holds true across different intervention methods including zeroing out, dampening, and mean replacement strategies.

G.1 Dampening

In their work, Suau et al. (2024) propose using a dampening function rather than setting neuron activations to zero outright. This approach, referred to as DAMP, corresponds to a specific choice of the intervention function $\phi(x) = \alpha x$, where $0 \leq \alpha \leq 1$. In this formulation, the activations of selected neurons are scaled down by a factor α instead of being completely suppressed. Here, x represents neuron activation. The rationale behind dampening is that a fixed intervention (like zeroing out) can disrupt the LLM's inference dynamics, especially when a large number of neurons (k) are involved, thereby limiting its effectiveness. Dampening offers a less destructive intervention by allowing contextual signals to continue passing through the network.

This, in turn, permits intervention on a larger set of expert neurons, potentially achieving stronger mitigation of the targeted concept.

Table 11 presents a comparative analysis of two intervention strategies, neuron masking and activation range masking, when employing the Dampening technique with $\alpha = 0.5$. The evaluation spans 14 classes and utilizes the metrics: accuracy (Acc), confidence (Conf), class-wise accuracy (CAcc), class-wise confidence (CConf), alterations in perplexity (PPL), and MMLU score.

A consistent trend emerges across the primary metrics (Acc, Conf, CAcc, and CConf), where activation range masking demonstrates superior performance over neuron masking. Interventions based on activation ranges lead to a notably smaller decline in the accuracy and confidence associated with auxiliary concepts. For example, in Class 3, while neuron masking results in an accuracy drop of -0.974 in the targeted class and auxiliary class accuracy decrease of -0.411, activation range masking, despite a comparable accuracy reduction in the targeted class (-0.970), shows a less severe impact on auxiliary class accuracy (-0.283). This pattern of activation range masking better preserves auxiliary class performance, is evident across all evaluated classes.

Examining the broader effects on language modeling capabilities reveals significant distinctions between the two approaches. Neuron masking results in a considerable rise in perplexity (PPL), with increases ranging from **+2.891 to +3.732** across all the classes. Furthermore, it tends to cause more pronounced negative shifts in MMLU scores, reaching as low as -0.045. Conversely, activation range masking results in substantially smaller increments in perplexity, falling within the **+0.546 to +0.810** range, and frequently results in improved or minimally altered MMLU scores, with gains up to +0.035.

G.2 Mean Replacement

Another approach of activation replacement discussed in the literature(Suau et al., 2021) is replacing it with the mean activation value. We provide the results for this type of replacement in Table 12.

The mean replacement strategy corresponds to setting the intervention function to $\phi(x) = \mu$, where μ is the mean activation of the neuron x computed over a general next-token prediction task on the Wikipedia (Foundation).

In Table 12, we assess the effect of mean replacement using both neuron masking and activation range masking. In every class, neuron masking results in more severe degradation than range-based masking across all auxiliary and general metrics.

Across metrics (Acc, Conf, CAcc, and CConf), activation range masking consistently outperforms neuron masking. The degradation in accuracy and confidence of auxiliary concepts is significantly lower under range-based interventions. For instance, in Class 3, neuron masking causes a drop of -1.000 in Acc and -0.766 in CAcc, whereas activation range masking yields a similar Acc drop (-1.000) but a substantially smaller decline in CAcc (-0.538). A similar pattern repeats across all classes; for example, in Class 0, neuron masking results in CAcc of -0.685 while activation range masking yields -0.551. In Class 7, neuron masking shows a CAcc of -0.491 compared to -0.267 for activation range masking.

Beyond auxiliary class performance, we observe substantial differences in how the two masking methods affect general language modelling capabilities. Neuron masking leads to a large increase in perplexity (PPL), ranging from **+7.413 to +8.791** which is catastrophic, across classes, and induces more negative shifts in MMLU scores (as low as -0.035 for Class 9, and also for Class 0 with -0.025, Class 1 with -0.030, Class 10 with -0.020, and Class 13 with -0.025). In contrast, activation range masking results in substantially smaller increases in perplexity (+0.397 to +0.687) and often yields improved or near-zero changes in MMLU scores (up to +0.020 for Class 6, and several positive values like +0.015 for Class 1, Class 8, and Class 9).

G.3 Adaptive Dampening

We propose a novel replacement method in which the intervention function $\phi(x)$ applies *runtime-controlled dampening* based on the distance of the observed activation x from the center of a predefined activation range. Specifically, the dampening factor $a(x)$ is linearly scaled according to the distance of x from the mean μ of the neuron's activation distribution, within the range $[\mu - 2.5\sigma, \mu + 2.5\sigma]$.

Let $\beta \in [0, 1]$ denote the maximum dampening factor applied at the range boundaries. Then:

$$a(x) = \beta \cdot \frac{|x - \mu|}{2.5\sigma}, \quad \text{and} \quad \phi(x) = a(x) \cdot x.$$

This ensures that when $x = \mu$ (the center of the range), $a(x) = 0$ and the activation is fully suppressed via $\phi(x) = 0$. At the boundaries ($x = \mu \pm 2.5\sigma$), $a(x) = \beta$, and the activation is minimally dampened. Values within the range are scaled proportionally based on their normalized distance from the mean. This adaptive dampening mechanism suppresses values near the mean while preserving those closer to the range edges.

The dampening factor β can be optimized for different neurons based on the concept information that neuron provides. For this work, we use $\beta = 0.5$ across all neurons.

In Table 13 we evaluate the adaptive dampening variant of the replacement function. This approach outperforms both neuron masking and static activation masking across all metrics.

In auxiliary class metrics, adaptive dampening yields much smaller degradation. Auxilary class accuracy (CAcc) and confidence (CConf) show significantly reduced drops compared to other methods. For example, in Class 0, CAcc drops only -0.215 compared to -0.685 under neuron masking and -0.551 under hard activation masking. The effect is consistent across classes, with most CAcc and CConf drops staying well below -0.3, and in many cases below -0.15.

Language modeling metrics show this approach to be exceptionally efficient. Perplexity increases are minimal, remaining within $+0.408$ to $+0.609$, substantially lower than all hard-masking variants. MMLU deltas also stay close to zero, with several classes showing improvement (e.g., Class 8: $+0.030$, Class 4: $+0.015$). Notably, no class suffers significant MMLU degradation.

H   Training Details

For BERT, DistilBERT, and Llama, we utilize pretrained models. Since BERT, and DistilBert are not inherently trained as a conversational agent, we use top-performing fine-tuned models from the Hugging Face repository. For the Llama model, few-shot prompt completion is employed to predict class labels. This involves providing a small number of training samples from the dataset to guide the model's predictions.

For GPT-2, we fine-tune the pretrained model across all datasets for three epochs. The input sequence is constructed by concatenating the text with a <sep> token, followed by the class label, and ending with an <eos> token. During training, the loss is back-propagated only for the class label token, while all other tokens are assigned a skip label (-100). Additionally, all class labels are added to the model's dictionary as special single-token entries.

In the case of Bert-based models, record the activation of the CLS token, In the case of GPT-2 and Llama models, we record the last token output when the class token is being predicted. The intervention is applied to the appropriate token on the residual stream.

For trained models (BERT, DistilBERT, and GPT-2), a higher proportion of neurons (up to 50%) can be ablated with a relatively minor impact on primary task performance and minimal interference with auxiliary concepts. This suggests substantial neuronal redundancy, wherein multiple neurons appear to encode overlapping features.

Dataset Preprocessing for Llama For Llama we process whole datasets in few shout settings and only curate 2000 samples per class, where the model prediction was correct.

H.1   Computation Details

All experiments, including activation extraction and interventions on large language models (LLMs), were conducted using an NVIDIA RTX 3090 GPU equipped with 24GB of VRAM. 64GB RAM.

I   Hyperparameter Ablation

The results for ablating τ on GPT-2 model using the X dataset are shown in Table 14. For target concept, values $0.3 - 2.4$ show decreasing accuracy/confidence, stabilizing at $\tau = 2.4$ (accuracy 0.6126). Beyond 2.4, negligible additional degradation occurs, indicating we've captured the complete target concept activation range. Importantly, while target performance stabilizes after $\tau = 2.4$, auxiliary task performance declines after $\tau = 2.7$. Complement accuracy stays above 0.93 until then before dropping to 0.8795 at $\tau = 4.5$. This aligns with normal distribution properties where 95-99% of values fall within ± 2.5 standard deviations.

J   Class Wise Results

Here we provide the complete results for the selected models for all datasets. IMDB (Table 16), SST2 (Table 17), AG-news (Table 15), Emotions (Table 18) and DBpedia-14 (Table 19)

Table 7: Full text for samples shown in Table2 for Neuron 1525 (Sci/Tech) and Neuron 2587 (Business).

Neuron	Point	Boundary Affinity	Representative Examples
1525	Lower Boundary	World / Sports	"Gene Tweaking Turns Couch Potato Mice Into Racers Altering a single gene turned ordinary mice into marathon racers that could run for hours and eat huge amounts of food without getting fat, a team of researchers reported on Monday." "Insecure elections marching ever closer Friday's St. Louis Post-Dispatch reports on a controversial decision by Missouri's Secretary of State: the state of Missouri will be allowing soldiers stationed overseas to cast ballots via e-mail. Their absentee ballots will be scanned and converted to PDF files, which will be emailed to the Defense Department, printed out, and then faxed to Missouri. I'm in favor of helping soldiers vote; this is a democracy, everyone should be able to vote. Yet I'm deeply skeptical of this proposal, for two reasons: The plan depends on e-mailed ballots being printed out and faxed by the Defense Department but does not provide any safeguards against soldiers being sanctioned for how they have voted; The transmission method is inherently technically insecure " "IBM's new supercomputer breaks the world's fastest computer's ... Technology India: London, Nov 8 : A new supercomputer being constructed by IBM has broken all supercomputing records after demonstrating double the power of the long-reigning supercomputing champion, NEC's Earth Simulator, based at Yokohama, Japan."
	Mean	Sci/Tech	"Sony, IBM, Toshiba say powerful chip to start production in 2005 SAN JOSE, Calif. A long-awaited microprocessor developed by IBM, Sony, and Toshiba will go into production next year and start appearing in video game consoles and high-definition T-Vs in 2006." "AMD Gives Details on Dual-Core Opteron Advanced Micro Devices has given out more details on its fortcoming dual-core microprocessor chip. The Opteron-based design is said to be 30-55 percent faster than AMD #39;s single-core chips, but it will fit in existing server designs." "Arm reveals Neon multimedia extension technology Microprocessor designer Arm Ltd. has developed a new multimedia technology called Neon that will help improve the performance of mobile electronics devices that process multiple tasks, the company said Monday."
	Upper Boundary	Business	"iPass Introduces New Flat-Rate Pricing Plans for US Wi-Fi Hotspot ... REDWOOD SHORES, Calif., Nov. 17 – iPass Inc. today announced new monthly and annual flat-rate subscription plans for use of the Company's US Wi-Fi connectivity." "NTT DoCoMo Rises on TSE on Reported Deal with Motorola Tokyo, Aug. 23 (Jiji Press)–NTT DoCoMo firmed on the Tokyo Stock Exchange Monday morning following a media report that it will start procuring mobile phone handsets made by Motorola Inc." "Update: Omnipod beefs up instant messaging service Omnipod, which provides hosted instant message (IM) services to companies of all sizes, is preparing several enhancements to its platform, including the additions of a Web-based client, a telephony component and a persistent-chat feature, Omnipod's chief executive officer said."
2587	Lower Boundary	World / Sports	"Put Me in, Coach! Coach joins the S P 500, and others stand to benefit from the leather in the weather." "London Stock Exchange eyes Asia HQ The London Stock Exchange plans to set up an Asia headquarters in Hong Kong to tap the growing number of mainland corporates eyeing listings abroad, a local newspaper reports." "Halliburton closes higher on Army's decision to pay DALLAS (CBS.MW) – Halliburton's shares closed higher Wednesday after the Army Materiel Command reversed its decision to withhold 15 percent of its future payments to the company under a contract to supply and support US troops in Iraq."
	Mean	Business	"UBS Buys Schwab Unit for $265 Mln GENEVA/NEW YORK (Reuters) - Swiss-based banking giant UBS AG has agreed to buy Charles Schwab Corp.'s capital markets unit for $265 million in cash, making UBS a leading player on the U.S. Nasdaq exchange, the companies said on Tuesday." "Applied Materials Applied Materials (AMAT: news, chart, profile) shares were off two cents to $16.05 in trading before the bell Wednesday and had wavered around break-even in late trading Tuesday after the results were announced." "Brown-Forman Earnings Jump 67 Percent Brown-Forman Corp. , which sells products ranging from Jack Daniels whiskey to Lenox china, on Thursday posted a better-than-expected 67 percent jump in earnings as aggressive marketing boosted sales of premium spirits and new wines."
	Upper Boundary	Sci/Tech	"Arm hands over $910m for US chip firm Arm is to pay $910m (504m) in cash and shares for Artisan, the US-based transistor-level designer for systems-on-a-chip. Arm chairman Sir Robin Saxby said in a conference call: quot;This will be a combination " "Oracle sales rise on database demand com September 14, 2004, 2:26 PM PT. This fourth priority's main focus has been improving or obtaining CRM and ERP software for the past year and a half." "Coming: IT that adapts to users' requirements The march of information technology into the workplace has been greeted with a mix of awe and resistance. For all their promise of productivity gains, computers, business software, and telecommunications gear have disrupted processes at the core of a company's identity."

Table 8: Statistical analysis of different layers showing skewness, kurtosis, and Kolmogorov- Smirnov test results. *GPT2* model. *AG-News Dataset*

Layer	Kurtosis	Skewness	Practical Normality
1	3.9314	0.0430	0.7913
2	3.7622	-0.0091	0.9525
3	3.4109	-0.0143	0.9870
4	3.5582	-0.0073	0.9801
5	3.6145	0.0051	0.9730
6	3.5318	0.0086	0.9769
7	3.3461	0.0083	0.9880
8	3.2763	0.0037	0.9870
9	3.2267	0.0039	0.9860
10	3.2057	0.0029	0.9899
11	3.2105	-0.0002	0.9912
12	3.2061	-0.0014	0.9919

Table 9: Evaluation of layer selection on *GPT-2* model on the *Emotions* dataset using neuron and range masking techniques. 20% Neurons selected. Here, **Acc** represents class accuracy, **Conf** denotes class prediction probability, and **CAcc** and **CConf** refer to average accuracy and average class prediction probability across other classes, respectively. The *Base Values* indicate the baseline model performance, while *Activation Range Masking* and *Neuron Masking* show deviations from the baseline performance.

Layer	Class	Base Values				Neuron Masking				Activation Range Masking			
		Acc	Conf	CAcc	CConf	Acc	Conf	CAcc	CConf	Acc	Conf	CAcc	CConf
1	Class 0	0.970	0.957	0.915	0.904	-0.029	-0.071	-0.074	-0.100	0.006	0.002	-0.004	-0.005
	Class 1	0.933	0.932	0.931	0.913	-0.011	-0.056	-0.090	-0.116	0.001	-0.003	-0.004	-0.004
	Class 2	0.901	0.865	0.934	0.924	-0.206	-0.195	-0.052	-0.092	-0.019	-0.015	-0.001	-0.002
	Class 3	0.926	0.924	0.932	0.919	-0.128	-0.152	-0.051	-0.090	-0.004	-0.005	-0.001	-0.002
	Class 4	0.885	0.867	0.938	0.927	-0.055	-0.084	-0.061	-0.093	-0.016	-0.009	0.002	-0.001
	Class 5	0.851	0.786	0.934	0.924	-0.249	-0.217	-0.055	-0.094	0.016	0.013	-0.004	-0.005
2	Class 0	0.970	0.957	0.915	0.904	-0.804	-0.808	-0.389	-0.386	-0.061	-0.133	-0.077	-0.096
	Class 1	0.933	0.932	0.931	0.913	0.053	-0.003	-0.819	-0.781	-0.011	-0.049	-0.110	-0.145
	Class 2	0.901	0.865	0.934	0.924	-0.868	-0.737	-0.515	-0.519	-0.365	-0.337	-0.077	-0.126
	Class 3	0.926	0.924	0.932	0.919	-0.870	-0.805	-0.498	-0.501	-0.215	-0.248	-0.096	-0.153
	Class 4	0.885	0.867	0.938	0.927	-0.729	-0.707	-0.461	-0.463	-0.042	-0.077	-0.076	-0.116
	Class 5	0.851	0.786	0.934	0.924	-0.845	-0.769	-0.511	-0.508	-0.229	-0.188	-0.106	-0.163
3	Class 0	0.970	0.957	0.915	0.904	-0.896	-0.904	-0.824	-0.832	-0.647	-0.688	-0.517	-0.544
	Class 1	0.933	0.932	0.931	0.913	-0.901	-0.916	-0.835	-0.832	-0.568	-0.607	-0.609	-0.630
	Class 2	0.901	0.865	0.934	0.924	-0.868	-0.845	-0.838	-0.851	-0.605	-0.600	-0.589	-0.619
	Class 3	0.926	0.924	0.932	0.919	-0.868	-0.896	-0.830	-0.840	-0.567	-0.605	-0.567	-0.596
	Class 4	0.885	0.867	0.938	0.927	-0.800	-0.811	-0.849	-0.857	-0.502	-0.522	-0.513	-0.544
	Class 5	0.851	0.786	0.934	0.924	0.022	0.081	-0.865	-0.881	-0.155	-0.124	-0.561	-0.596
4	Class 0	0.970	0.957	0.915	0.904	-0.650	-0.703	-0.698	-0.764	-0.608	-0.621	-0.499	-0.510
	Class 1	0.933	0.932	0.931	0.913	-0.845	-0.884	-0.667	-0.725	-0.491	-0.519	-0.480	-0.491
	Class 2	0.901	0.865	0.934	0.924	-0.858	-0.824	-0.772	-0.809	-0.488	-0.497	-0.506	-0.523
	Class 3	0.926	0.924	0.932	0.919	-0.700	-0.808	-0.663	-0.739	-0.534	-0.546	-0.512	-0.528
	Class 4	0.885	0.867	0.938	0.927	-0.239	-0.514	-0.754	-0.797	-0.304	-0.307	-0.452	-0.471
	Class 5	0.851	0.786	0.934	0.924	-0.612	-0.463	-0.692	-0.765	-0.047	-0.038	-0.525	-0.541
5	Class 0	0.970	0.957	0.915	0.904	-0.838	-0.852	-0.492	-0.630	-0.695	-0.688	-0.554	-0.555
	Class 1	0.933	0.932	0.931	0.913	-0.387	-0.563	-0.683	-0.714	-0.552	-0.564	-0.605	-0.599
	Class 2	0.901	0.865	0.934	0.924	-0.702	-0.700	-0.634	-0.690	-0.472	-0.470	-0.607	-0.605
	Class 3	0.926	0.924	0.932	0.919	-0.361	-0.507	-0.615	-0.692	-0.567	-0.575	-0.538	-0.539
	Class 4	0.885	0.867	0.938	0.927	-0.873	-0.844	-0.525	-0.650	-0.668	-0.653	-0.594	-0.594
	Class 5	0.851	0.786	0.934	0.924	-0.637	-0.573	-0.588	-0.681	-0.069	-0.022	-0.548	-0.553
6	Class 0	0.970	0.957	0.915	0.904	-0.720	-0.775	-0.829	-0.830	-0.484	-0.499	-0.318	-0.322
	Class 1	0.933	0.932	0.931	0.913	-0.871	-0.887	-0.750	-0.768	-0.176	-0.195	-0.499	-0.499
	Class 2	0.901	0.865	0.934	0.924	-0.895	-0.860	-0.735	-0.773	-0.680	-0.638	-0.335	-0.348
	Class 3	0.926	0.924	0.932	0.919	-0.863	-0.884	-0.772	-0.793	-0.418	-0.431	-0.379	-0.381
	Class 4	0.885	0.867	0.938	0.927	-0.621	-0.669	-0.743	-0.784	-0.430	-0.435	-0.247	-0.262
	Class 5	0.851	0.786	0.934	0.924	-0.143	-0.086	-0.808	-0.831	-0.114	-0.070	-0.474	-0.478

Table 10: Evaluation of layer selection on *GPT-2* model on the *Emotions* dataset using neuron and range masking techniques. 20% Neurons selected. Here, **Acc** represents class accuracy, **Conf** denotes class prediction probability, and **CAcc** and **CConf** refer to average accuracy and average class prediction probability across other classes, respectively. The *Base Values* indicate the baseline model performance, while *Activation Range Masking* and *Neuron Masking* show deviations from the baseline performance.

Layer	Class	Base Values				Neuron Masking				Activation Range Masking			
		Acc	Conf	CAcc	CConf	Acc	Conf	CAcc	CConf	Acc	Conf	CAcc	CConf
7	Class 0	0.970	0.957	0.915	0.904	-0.908	-0.901	-0.752	-0.753	-0.527	-0.538	-0.492	-0.498
	Class 1	0.933	0.932	0.931	0.913	-0.884	-0.895	-0.743	-0.729	-0.484	-0.509	-0.330	-0.338
	Class 2	0.901	0.865	0.934	0.924	-0.866	-0.835	-0.767	-0.765	-0.451	-0.442	-0.336	-0.355
	Class 3	0.926	0.924	0.932	0.919	-0.786	-0.819	-0.641	-0.666	-0.445	-0.457	-0.331	-0.346
	Class 4	0.885	0.867	0.938	0.927	-0.626	-0.618	-0.810	-0.817	-0.341	-0.335	-0.521	-0.532
	Class 5	0.851	0.786	0.934	0.924	0.106	0.147	-0.810	-0.811	0.102	0.107	-0.547	-0.553
8	Class 0	0.970	0.957	0.915	0.904	-0.776	-0.791	-0.209	-0.291	-0.191	-0.312	-0.082	-0.114
	Class 1	0.933	0.932	0.931	0.913	-0.585	-0.667	-0.412	-0.441	-0.591	-0.644	-0.199	-0.227
	Class 2	0.901	0.865	0.934	0.924	-0.692	-0.716	-0.469	-0.496	-0.560	-0.562	-0.468	-0.486
	Class 3	0.926	0.924	0.932	0.919	-0.657	-0.714	-0.415	-0.464	-0.468	-0.503	-0.230	-0.266
	Class 4	0.885	0.867	0.938	0.927	-0.501	-0.509	-0.531	-0.569	-0.201	-0.234	-0.258	-0.290
	Class 5	0.851	0.786	0.934	0.924	-0.092	-0.050	-0.634	-0.647	0.065	0.058	-0.279	-0.308
9	Class 0	0.970	0.957	0.915	0.904	-0.759	-0.768	-0.311	-0.351	-0.610	-0.661	-0.307	-0.328
	Class 1	0.933	0.932	0.931	0.913	-0.570	-0.713	-0.319	-0.346	-0.906	-0.910	-0.267	-0.298
	Class 2	0.901	0.865	0.934	0.924	-0.424	-0.520	-0.504	-0.531	-0.635	-0.643	-0.579	-0.595
	Class 3	0.926	0.924	0.932	0.919	-0.810	-0.834	-0.501	-0.502	-0.759	-0.772	-0.502	-0.516
	Class 4	0.885	0.867	0.938	0.927	-0.358	-0.357	-0.476	-0.481	-0.587	-0.566	-0.519	-0.527
	Class 5	0.851	0.786	0.934	0.924	-0.133	-0.101	-0.546	-0.554	0.106	0.104	-0.450	-0.462
10	Class 0	0.970	0.957	0.915	0.904	-0.733	-0.741	-0.105	-0.126	-0.624	-0.659	-0.146	-0.163
	Class 1	0.933	0.932	0.931	0.913	-0.389	-0.671	-0.178	-0.209	-0.899	-0.911	-0.254	-0.285
	Class 2	0.901	0.865	0.934	0.924	-0.230	-0.513	-0.116	-0.224	-0.699	-0.735	-0.409	-0.451
	Class 3	0.926	0.924	0.932	0.919	-0.434	-0.687	-0.081	-0.133	-0.898	-0.905	-0.401	-0.455
	Class 4	0.885	0.867	0.938	0.927	-0.489	-0.506	-0.188	-0.256	-0.140	-0.186	-0.063	-0.102
	Class 5	0.851	0.786	0.934	0.924	-0.306	-0.243	-0.157	-0.240	0.063	0.010	-0.095	-0.127
11	Class 0	0.970	0.957	0.915	0.904	-0.358	-0.496	-0.382	-0.414	-0.301	-0.441	-0.121	-0.148
	Class 1	0.933	0.932	0.931	0.913	-0.800	-0.857	-0.078	-0.123	-0.858	-0.875	-0.128	-0.162
	Class 2	0.901	0.865	0.934	0.924	-0.897	-0.861	-0.416	-0.450	-0.901	-0.864	-0.464	-0.500
	Class 3	0.926	0.924	0.932	0.919	-0.923	-0.921	-0.427	-0.470	-0.913	-0.914	-0.354	-0.393
	Class 4	0.885	0.867	0.938	0.927	-0.152	-0.212	-0.039	-0.075	-0.210	-0.239	-0.181	-0.204
	Class 5	0.851	0.786	0.934	0.924	0.047	-0.028	-0.131	-0.173	0.053	0.002	-0.142	-0.159
12	Class 0	0.970	0.957	0.915	0.904	-0.550	-0.603	-0.013	-0.003	-0.542	-0.594	0.005	0.012
	Class 1	0.933	0.932	0.931	0.913	-0.526	-0.545	0.001	0.012	-0.521	-0.538	-0.005	-0.004
	Class 2	0.901	0.865	0.934	0.924	-0.416	-0.402	0.002	0.006	-0.419	-0.407	0.007	0.006
	Class 3	0.926	0.924	0.932	0.919	-0.561	-0.576	-0.007	0.003	-0.561	-0.572	0.000	0.005
	Class 4	0.885	0.867	0.938	0.927	-0.655	-0.658	-0.042	-0.034	-0.657	-0.659	-0.011	-0.003
	Class 5	0.851	0.786	0.934	0.924	-0.718	-0.672	-0.300	-0.297	-0.718	-0.672	-0.267	-0.266

Table 11: **Dampening intervention results** on Llama-3.2-3B (DBPedia-14): comparison of neuron and range masking. 30% neurons were selected. Dampening factor used is $a = 0.125$. **Acc** represents class accuracy, **Conf** denotes class prediction probability, and **CAcc** and **CConf** refer to average accuracy and average class prediction probability across other classes, respectively. The *Base Values* indicate the baseline model performance, while *Neuron Masking* and *Activation Range Masking* show deviations from the baseline performance. PPL Δ and MMLU Δ show changes in perplexity and MMLU scores, respectively.

Class	Base Values				Neuron Masking						Activation Range Masking					
	Acc	Conf	CAcc	CConf	Acc	Conf	CAcc	CConf	PPL Δ	MMLU Δ	Acc	Conf	CAcc	CConf	PPL Δ	MMLU Δ
Class 0	1.000	0.576	1.000	0.563	-0.919	-0.545	-0.281	-0.309	3.161	-0.020	-0.924	-0.545	**-0.276**	**-0.285**	**0.640**	**-0.010**
Class 1	1.000	0.526	1.000	0.567	-0.988	-0.467	-0.246	-0.270	3.578	-0.015	-0.805	-0.466	**-0.193**	**-0.206**	**0.725**	**0.015**
Class 2	1.000	0.441	1.000	0.575	-0.864	-0.391	-0.461	-0.323	2.891	-0.030	-0.869	-0.389	**-0.346**	**-0.282**	**0.718**	**0.005**
Class 3	1.000	0.461	1.000	0.573	-0.974	-0.439	-0.411	-0.346	3.036	-0.025	-0.970	-0.438	**-0.282**	**-0.283**	**0.653**	**0.010**
Class 4	1.000	0.839	1.000	0.541	-0.382	-0.597	-0.367	-0.317	2.997	0.000	-0.382	-0.597	**-0.334**	**-0.284**	**0.691**	**0.020**
Class 5	1.000	0.339	1.000	0.568	-0.970	-0.326	-0.239	-0.246	3.503	0.010	-0.970	-0.325	**-0.197**	**-0.187**	**0.810**	**0.015**
Class 6	1.000	0.810	1.000	0.545	-0.233	-0.638	-0.194	-0.276	3.126	-0.010	-0.241	-0.637	**-0.174**	**-0.203**	**0.697**	-0.010
Class 7	1.000	0.595	1.000	0.562	-0.210	-0.382	-0.206	-0.226	3.037	0.000	-0.179	-0.376	**-0.123**	**-0.143**	**0.546**	**0.015**
Class 8	1.000	0.417	1.000	0.574	-0.310	-0.416	-0.335	-0.297	3.001	0.020	-0.346	-0.416	**-0.200**	**-0.187**	**0.624**	**0.015**
Class 9	1.000	0.526	1.000	0.567	-0.820	-0.465	-0.327	-0.264	3.369	-0.030	-0.809	-0.463	**-0.213**	**-0.189**	**0.596**	**0.000**
Class 10	1.000	0.505	1.000	0.569	-0.691	-0.466	-0.389	-0.314	3.732	**0.000**	-0.696	-0.465	**-0.267**	**-0.198**	**0.695**	-0.015
Class 11	1.000	0.497	1.000	0.569	-0.873	-0.432	-0.472	-0.289	3.070	-0.030	-0.865	-0.427	**-0.205**	**-0.205**	**0.594**	**-0.015**
Class 12	1.000	0.573	1.000	0.563	-0.720	-0.452	-0.295	-0.221	3.410	-0.045	-0.723	-0.451	**-0.190**	**-0.163**	**0.595**	**0.035**
Class 13	1.000	0.567	1.000	0.564	-0.951	-0.537	-0.226	-0.189	2.995	0.000	-0.955	-0.536	**-0.157**	**-0.150**	**0.672**	**0.005**

Table 12: **Mean replacement intervention** results on Llama-3.2-3B (DBPedia-14): comparison of neuron and range masking.. 30% neurons were selected 30% neurons were selected. Mean Activation μ is used as replacement value. **Acc** represents class accuracy, **Conf** denotes class prediction probability, and **CAcc** and **CConf** refer to average accuracy and average class prediction probability across other classes, respectively. The *Base Values* indicate the baseline model performance, while *Neuron Masking* and *Activation Range Masking* show deviations from the baseline performance. PPL Δ and MMLU Δ show changes in perplexity and MMLU scores, respectively.

Class	Base Values				Neuron Masking						Activation Range Masking					
	Acc	Conf	CAcc	CConf	Acc	Conf	CAcc	CConf	PPL Δ	MMLU Δ	Acc	Conf	CAcc	CConf	PPL Δ	MMLU Δ
Class 0	1.000	0.576	1.000	0.563	-1.000	-0.576	-0.685	-0.554	7.681	-0.025	-1.000	-0.576	**-0.551**	**-0.545**	**0.687**	**-0.005**
Class 1	1.000	0.526	1.000	0.567	-1.000	-0.526	-0.554	-0.550	8.437	-0.030	-1.000	-0.526	**-0.356**	**-0.517**	**0.583**	**0.015**
Class 2	1.000	0.441	1.000	0.575	-0.995	-0.441	-0.697	-0.556	7.567	-0.015	-0.995	-0.440	**-0.574**	**-0.536**	**0.520**	**-0.010**
Class 3	1.000	0.461	1.000	0.573	-1.000	-0.461	-0.766	-0.561	8.005	-0.015	-1.000	-0.461	**-0.538**	**-0.534**	**0.543**	**0.010**
Class 4	1.000	0.839	1.000	0.541	-1.000	-0.838	-0.724	-0.528	8.239	**0.010**	-0.995	-0.838	**-0.502**	**-0.503**	**0.565**	0.005
Class 5	1.000	0.339	1.000	0.568	-1.000	-0.339	-0.616	-0.551	7.753	**0.010**	-1.000	-0.339	**-0.382**	**-0.510**	**0.552**	0.005
Class 6	1.000	0.810	1.000	0.545	-0.313	-0.805	-0.549	-0.531	7.880	-0.005	-0.292	-0.805	**-0.336**	**-0.499**	**0.547**	**0.020**
Class 7	1.000	0.595	1.000	0.562	-1.000	-0.592	-0.491	-0.535	7.413	-0.010	-0.995	-0.591	**-0.267**	**-0.449**	**0.462**	**0.000**
Class 8	1.000	0.417	1.000	0.574	-0.928	-0.414	-0.632	-0.556	7.688	0.015	-0.934	-0.414	**-0.298**	**-0.489**	**0.495**	0.015
Class 9	1.000	0.526	1.000	0.567	-1.000	-0.526	-0.611	-0.544	8.057	-0.035	-1.000	-0.526	**-0.370**	**-0.482**	**0.467**	**0.015**
Class 10	1.000	0.505	1.000	0.569	-0.998	-0.505	-0.642	-0.558	8.791	-0.020	-0.998	-0.505	**-0.406**	**-0.485**	**0.484**	0.005
Class 11	1.000	0.497	1.000	0.569	-1.000	-0.497	-0.719	-0.543	7.903	**0.025**	-1.000	-0.497	**-0.447**	**-0.459**	**0.397**	-0.005
Class 12	1.000	0.573	1.000	0.563	-0.904	-0.572	-0.629	-0.543	8.046	-0.005	-0.896	-0.571	**-0.375**	**-0.484**	**0.425**	**0.000**
Class 13	1.000	0.567	1.000	0.564	-1.000	-0.566	-0.526	-0.533	7.543	-0.025	-0.998	-0.566	**-0.341**	**-0.481**	**0.464**	**-0.010**

Table 13: Adaptive dampening intervention results on Llama-3.2-3B (DBPedia-14): comparison of neuron and range masking.. 30% neurons were selected. Adaptive Dampening factor used is $\beta = 0.5$. **Acc** represents class accuracy, **Conf** denotes class prediction probability, and **CAcc** and **CConf** refer to average accuracy and average class prediction probability across other classes, respectively. The *Base Values* indicate the baseline model performance, while *Neuron Masking* and *Activation Range Masking* show deviations from the baseline performance. PPL Δ and MMLU Δ show changes in perplexity and MMLU scores, respectively.

Class	Base Values				Activation Range Masking					
	Acc	Conf	CAcc	CConf	Acc	Conf	CAcc	CConf	PPL Δ	MMLU Δ
Class 0	1.000	0.576	1.000	0.563	-0.927	-0.543	-0.215	-0.217	0.487	-0.015
Class 1	1.000	0.526	1.000	0.567	-0.791	-0.451	-0.134	-0.109	0.543	0.000
Class 2	1.000	0.441	1.000	0.575	-0.828	-0.380	-0.277	-0.215	0.540	-0.010
Class 3	1.000	0.461	1.000	0.573	-0.958	-0.432	-0.230	-0.214	0.492	0.010
Class 4	1.000	0.839	1.000	0.541	-0.346	-0.579	-0.261	-0.218	0.521	0.015
Class 5	1.000	0.339	1.000	0.568	-0.960	-0.319	-0.140	-0.116	0.609	-0.015
Class 6	1.000	0.810	1.000	0.545	-0.236	-0.613	-0.130	-0.122	0.524	-0.010
Class 7	1.000	0.595	1.000	0.562	-0.243	-0.388	-0.108	-0.080	0.408	0.005
Class 8	1.000	0.417	1.000	0.574	-0.440	-0.414	-0.152	-0.088	0.465	0.030
Class 9	1.000	0.526	1.000	0.567	-0.799	-0.459	-0.182	-0.131	0.445	0.005
Class 10	1.000	0.505	1.000	0.569	-0.684	-0.451	-0.222	-0.130	0.513	-0.010
Class 11	1.000	0.497	1.000	0.569	-0.836	-0.420	-0.308	-0.155	0.440	-0.005
Class 12	1.000	0.573	1.000	0.563	-0.720	-0.451	-0.172	-0.095	0.444	0.025
Class 13	1.000	0.567	1.000	0.564	-0.941	-0.530	-0.142	-0.098	0.502	0.010

Table 14: Performance metrics for varying τ values.

τ	Acc	Conf	CAcc	CConf
0.3	0.9021	0.8858	0.9452	0.9358
0.6	0.8439	0.8185	0.9424	0.9327
0.9	0.7801	0.7486	0.9391	0.9263
1.2	0.7295	0.6950	0.9340	0.9174
1.5	0.6834	0.6482	0.9337	0.9093
1.8	0.6424	0.6141	0.9331	0.9000
2.1	0.6184	0.5926	0.9327	0.8910
2.4	0.6126	0.5858	0.9314	0.8846
2.7	0.6024	0.5798	0.9280	0.8800
3.0	0.5971	0.5776	0.9234	0.8777
3.3	0.5963	0.5786	0.9173	0.8753
3.6	0.5970	0.5794	0.9097	0.8729
3.9	0.5976	0.5802	0.9020	0.8698
4.2	0.5967	0.5798	0.8908	0.8642
4.5	0.5967	0.5798	0.8795	0.8577

Table 15: Evaluation of selected models on the *AG-News* dataset using neuron and range masking techniques. **Acc** represents class accuracy, **Conf** denotes class prediction probability, and **CAcc** and **CConf** refer to average accuracy and average class prediction probability across other classes, respectively. The *Base Values* indicate the baseline model performance, while *Activation Range Masking* and *Neuron Masking* show deviations from the baseline performance. For *GPT-2* 50% and for *Llama-3.2-3B* 30% neurons selected.

Model	Class	Base Values				Neuron Masking				Activation Range Masking			
		Acc	Conf	CAcc	CConf	Acc	Conf	CAcc	CConf	Acc	Conf	CAcc	CConf
BERT	Class 0	0.945	0.936	0.949	0.927	-0.205	-0.587	**0.004**	-0.076	-0.198	-0.589	0.007	**-0.010**
	Class 1	0.993	0.988	0.933	0.910	-0.225	-0.659	0.004	-0.077	-0.194	-0.650	**0.003**	**-0.012**
	Class 2	0.905	0.881	0.962	0.945	-0.300	-0.536	0.014	-0.079	-0.298	-0.542	0.014	**-0.009**
	Class 3	0.949	0.913	0.948	0.935	-0.354	-0.577	0.026	-0.065	-0.353	-0.579	**0.025**	**-0.005**
GPT-2	Class 0	0.955	0.951	0.941	0.928	-0.920	-0.926	-0.231	-0.224	-0.919	-0.925	**-0.019**	**-0.008**
	Class 1	0.986	0.981	0.931	0.917	-0.926	-0.931	-0.253	-0.257	-0.912	-0.916	**-0.054**	**-0.069**
	Class 2	0.897	0.886	0.960	0.949	-0.696	-0.737	-0.110	**-0.132**	-0.678	-0.725	**-0.097**	-0.306
	Class 3	0.940	0.916	0.946	0.939	-0.940	-0.916	-0.024	**-0.037**	-0.887	-0.882	**-0.080**	-0.510
Llama-3.2-3B	Class 0	1.000	0.936	1.000	0.680	-0.995	-0.934	-0.530	-0.427	-0.995	-0.934	**-0.345**	**-0.306**
	Class 1	1.000	0.742	1.000	0.744	-0.870	-0.680	-0.615	-0.599	-0.875	-0.681	**-0.515**	**-0.503**
	Class 2	1.000	0.655	1.000	0.773	-0.895	-0.646	-0.795	-0.634	-0.895	-0.646	**-0.655**	**-0.549**
	Class 3	1.000	0.642	1.000	0.778	-0.975	-0.641	-0.698	-0.630	-0.975	-0.640	**-0.420**	**-0.459**

Table 16: Evaluation of selected models on the *IMDB* dataset using neuron and range masking techniques. Here, **Acc** represents class accuracy, **Conf** denotes class prediction probability, and **CAcc** and **CConf** refer to average accuracy and average class prediction probability across other classes, respectively. The *Base Values* indicate the baseline model performance, while *Activation Range Masking* and *Neuron Masking* show deviations from the baseline performance.

Model	Class	Base Values				Neuron Masking				Activation Range Masking			
		Acc	Conf	CAcc	CConf	Acc	Conf	CAcc	CConf	Acc	Conf	CAcc	CConf
BERT	Class 0	0.930	0.908	0.926	0.901	-0.169	-0.352	0.061	-0.066	-0.163	-0.359	0.059	0.035
	Class 1	0.926	0.901	0.930	0.908	-0.211	-0.355	0.057	-0.091	-0.206	-0.361	0.056	0.025
GPT-2	Class 0	0.965	0.941	0.940	0.922	-0.935	-0.922	0.050	0.057	-0.905	-0.901	0.055	0.046
	Class 1	0.940	0.922	0.965	0.941	-0.620	-0.667	0.005	0.018	-0.610	-0.657	0.015	0.027
Llama-3.2-3B	Class 0	1.000	0.619	1.000	0.500	-0.643	-0.448	-0.515	-0.287	-0.640	-0.446	-0.502	-0.278
	Class 1	1.000	0.500	1.000	0.619	-0.877	-0.410	-0.273	-0.304	-0.873	-0.409	-0.265	-0.303

Table 17: Evaluation of selected models on the *SST2* dataset using neuron and range masking techniques. Here, **Acc** represents class accuracy, **Conf** denotes class prediction probability, and **CAcc** and **CConf** refer to average accuracy and average class prediction probability across other classes, respectively. The *Base Values* indicate the baseline model performance, while *Activation Range Masking* and *Neuron Masking* show deviations from the baseline performance.

Model	Class	Base Values				Neuron Masking				Activation Range Masking			
		Acc	Conf	CAcc	CConf	Acc	Conf	CAcc	CConf	Acc	Conf	CAcc	CConf
BERT	Class 0	0.890	0.882	0.930	0.925	-0.058	-0.308	0.029	-0.047	-0.075	-0.329	0.031	0.036
	Class 1	0.930	0.925	0.890	0.882	-0.043	-0.318	0.033	-0.045	-0.045	-0.330	0.030	0.050
GPT-2	Class 0	0.950	0.937	0.981	0.978	-0.142	-0.158	0.010	0.012	-0.142	-0.167	0.009	0.010
	Class 1	0.981	0.978	0.950	0.937	-0.187	-0.223	0.041	0.053	-0.176	-0.216	0.041	0.046
Llama-3.2-3B	Class 0	1.000	0.620	1.000	0.690	-0.532	-0.459	-0.420	-0.424	-0.532	-0.456	-0.404	-0.415
	Class 1	1.000	0.690	1.000	0.620	-0.289	-0.379	-0.326	-0.315	-0.284	-0.376	-0.306	-0.301

Table 18: Evaluation of selected models on the *Emotions* dataset using neuron and range masking techniques. Here, **Acc** represents class accuracy, **Conf** denotes class prediction probability, and **CAcc** and **CConf** refer to average accuracy and average class prediction probability across other classes, respectively. The *Base Values* indicate the baseline model performance, while *Activation Range Masking* and *Neuron Masking* show deviations from the baseline performance.

Model	Class	Base Values				Neuron Masking				Activation Range Masking			
		Acc	Conf	CAcc	CConf	Acc	Conf	CAcc	CConf	Acc	Conf	CAcc	CConf
BERT	Class 0	0.960	0.935	0.901	0.851	-0.241	-0.718	0.013	-0.266	-0.222	-0.718	0.012	-0.055
	Class 1	0.942	0.904	0.905	0.861	-0.223	-0.691	0.028	-0.254	-0.213	-0.692	0.032	-0.064
	Class 2	0.824	0.723	0.926	0.889	-0.371	-0.533	0.016	-0.284	-0.352	-0.534	0.018	-0.115
	Class 3	0.927	0.873	0.916	0.876	-0.247	-0.664	0.010	-0.256	-0.240	-0.667	0.012	-0.057
	Class 4	0.884	0.837	0.922	0.880	-0.406	-0.646	0.012	-0.251	-0.402	-0.648	0.012	-0.066
	Class 5	0.591	0.566	0.929	0.886	-0.303	-0.392	0.004	-0.299	-0.303	-0.397	0.005	-0.090
GPT-2	Class 0	0.969	0.956	0.913	0.903	-0.695	-0.751	-0.125	-0.124	-0.698	-0.749	-0.009	-0.009
	Class 1	0.939	0.938	0.925	0.908	-0.879	-0.882	-0.019	-0.009	-0.879	-0.880	-0.016	-0.015
	Class 2	0.902	0.872	0.932	0.923	-0.776	-0.736	-0.029	-0.032	-0.780	-0.739	-0.023	-0.028
	Class 3	0.910	0.905	0.932	0.921	-0.713	-0.714	-0.006	-0.007	-0.715	-0.716	-0.002	-0.001
	Class 4	0.869	0.854	0.938	0.927	-0.754	-0.753	-0.240	-0.248	-0.754	-0.753	-0.127	-0.133
	Class 5	0.857	0.798	0.932	0.923	-0.587	-0.601	-0.301	-0.308	-0.587	-0.601	-0.280	-0.289
Llama-3.2-3B	Class 0	0.950	0.550	0.782	0.455	-0.950	-0.547	-0.655	-0.408	-0.945	-0.547	-0.571	-0.378
	Class 1	0.905	0.498	0.804	0.473	-0.855	-0.495	-0.743	-0.433	-0.867	-0.494	-0.607	-0.404
	Class 2	0.785	0.421	0.827	0.483	-0.785	-0.420	-0.771	-0.454	-0.785	-0.420	-0.658	-0.436
	Class 3	0.790	0.482	0.833	0.476	-0.760	-0.477	-0.635	-0.423	-0.755	-0.476	-0.544	-0.402
	Class 4	0.780	0.487	0.829	0.476	-0.780	-0.486	-0.534	-0.365	-0.780	-0.486	-0.444	-0.324
	Class 5	0.536	0.296	0.855	0.498	-0.417	-0.284	-0.751	-0.465	-0.429	-0.282	-0.653	-0.434

Table 19: Evaluation of selected models on the *DBPedia-14* dataset using neuron and range masking techniques. Here, **Acc** represents class accuracy, **Conf** denotes class prediction probability, and **CAcc** and **CConf** refer to average accuracy and average class prediction probability across other classes, respectively. The *Base Values* indicate the baseline model performance, while *Activation Range Masking* and *Neuron Masking* show deviations from the baseline performance.

Model	Class	Base Values				Neuron Masking				Activation Range Masking			
		Acc	Conf	CAcc	CConf	Acc	Conf	CAcc	CConf	Acc	Conf	CAcc	CConf
BERT	Class 0	0.972	0.966	0.992	0.991	-0.082	-0.702	0.001	-0.014	-0.076	-0.698	0.001	-0.000
	Class 1	0.987	0.986	0.991	0.990	-0.030	-0.778	0.000	-0.017	-0.018	-0.770	0.000	-0.000
	Class 2	0.987	0.985	0.991	0.990	-0.239	-0.814	0.001	-0.018	-0.217	-0.806	0.001	-0.000
	Class 3	0.997	0.997	0.990	0.989	-0.008	-0.766	0.000	-0.019	-0.001	-0.731	0.000	-0.000
	Class 4	0.984	0.983	0.991	0.990	-0.058	-0.777	0.001	-0.018	-0.032	-0.761	0.000	-0.000
	Class 5	0.995	0.995	0.990	0.989	-0.007	-0.795	0.000	-0.017	-0.001	-0.771	0.000	-0.000
	Class 6	0.975	0.974	0.992	0.991	-0.121	-0.807	0.000	-0.015	-0.112	-0.803	0.000	-0.001
	Class 7	0.994	0.994	0.990	0.989	-0.028	-0.789	0.000	-0.017	-0.010	-0.767	0.000	-0.000
	Class 8	1.000	1.000	0.990	0.989	-0.001	-0.808	0.000	-0.022	0.000	-0.772	0.000	-0.000
	Class 9	0.999	0.998	0.990	0.989	-0.004	-0.837	0.000	-0.019	-0.001	-0.811	0.000	-0.000
	Class 10	0.994	0.993	0.990	0.989	-0.025	-0.846	0.000	-0.016	-0.005	-0.831	0.000	-0.000
	Class 11	0.997	0.997	0.990	0.989	-0.013	-0.751	0.000	-0.017	-0.001	-0.726	0.000	-0.000
	Class 12	0.990	0.990	0.990	0.989	-0.018	-0.772	0.000	-0.017	-0.005	-0.755	0.000	-0.000
	Class 13	0.994	0.994	0.990	0.989	-0.009	-0.740	0.001	-0.017	-0.001	-0.721	0.000	-0.000
GPT-2	Class 0	0.985	0.977	0.990	0.989	-0.860	-0.877	-0.133	-0.136	-0.850	-0.869	-0.002	-0.017
	Class 1	0.995	0.992	0.990	0.988	-0.500	-0.567	-0.180	-0.192	-0.460	-0.544	-0.023	-0.024
	Class 2	0.985	0.980	0.990	0.989	-0.890	-0.904	-0.189	-0.213	-0.880	-0.902	-0.004	-0.010
	Class 3	0.995	0.995	0.990	0.987	-0.900	-0.933	-0.145	-0.143	-0.900	-0.927	-0.008	-0.017
	Class 4	0.970	0.969	0.992	0.989	-0.715	-0.773	-0.224	-0.260	-0.695	-0.750	-0.042	-0.062
	Class 5	0.995	0.993	0.990	0.988	-0.315	-0.446	-0.127	-0.192	-0.290	-0.432	-0.013	-0.025
	Class 6	0.965	0.964	0.992	0.990	-0.925	-0.932	-0.052	-0.062	-0.910	-0.928	-0.006	-0.007
	Class 7	1.000	0.998	0.989	0.987	-0.815	-0.865	-0.003	-0.008	-0.775	-0.846	-0.026	-0.057
	Class 8	1.000	1.000	0.989	0.987	-0.995	-0.990	-0.148	-0.188	-0.900	-0.932	-0.026	-0.055
	Class 9	1.000	1.000	0.989	0.987	-0.975	-0.979	-0.250	-0.268	-0.955	-0.958	-0.020	-0.049
	Class 10	0.995	0.993	0.990	0.988	-0.595	-0.685	-0.045	-0.053	-0.590	-0.675	-0.005	-0.011
	Class 11	0.985	0.984	0.990	0.988	-0.210	-0.453	-0.094	-0.118	-0.135	-0.396	-0.015	-0.034
	Class 12	0.990	0.988	0.990	0.988	-0.930	-0.938	-0.293	-0.309	-0.855	-0.880	-0.013	-0.029
	Class 13	1.000	0.999	0.989	0.987	-0.985	-0.986	-0.393	-0.416	-0.945	-0.981	-0.018	-0.044
Llama-3.2-3B	Class 0	1.000	0.586	1.000	0.559	-0.990	-0.584	-0.949	-0.473	-0.990	-0.584	-0.823	-0.441
	Class 1	1.000	0.533	1.000	0.563	-1.000	-0.528	-0.870	-0.446	-0.970	-0.528	-0.706	-0.371
	Class 2	1.000	0.467	1.000	0.568	-0.995	-0.462	-0.963	-0.477	-0.995	-0.461	-0.838	-0.432
	Class 3	1.000	0.460	1.000	0.569	-0.995	-0.459	-0.981	-0.486	-0.995	-0.459	-0.815	-0.420
	Class 4	1.000	0.828	1.000	0.539	-0.965	-0.809	-0.981	-0.454	-0.955	-0.808	-0.852	-0.412
	Class 5	1.000	0.349	1.000	0.568	-1.000	-0.348	-0.882	-0.429	-0.989	-0.347	-0.585	-0.346
	Class 6	1.000	0.809	1.000	0.541	-1.000	-0.787	-0.972	-0.449	-1.000	-0.787	-0.736	-0.366
	Class 7	1.000	0.599	1.000	0.558	-0.855	-0.588	-0.918	-0.410	-0.860	-0.586	-0.489	-0.274
	Class 8	1.000	0.420	1.000	0.572	-1.000	-0.420	-0.957	-0.467	-1.000	-0.420	-0.660	-0.335
	Class 9	1.000	0.527	1.000	0.563	-1.000	-0.524	-0.842	-0.435	-0.995	-0.523	-0.552	-0.320
	Class 10	1.000	0.505	1.000	0.565	-0.995	-0.503	-0.907	-0.464	-1.000	-0.503	-0.589	-0.322
	Class 11	1.000	0.505	1.000	0.565	-0.975	-0.501	-0.862	-0.416	-0.970	-0.501	-0.579	-0.313
	Class 12	1.000	0.560	1.000	0.561	-0.980	-0.545	-0.812	-0.417	-0.975	-0.544	-0.496	-0.310
	Class 13	1.000	0.587	1.000	0.559	-0.990	-0.584	-0.722	-0.406	-0.985	-0.584	-0.588	-0.337